Modelling and improved design of a displacement converter for a thin sound source

University of Twente
Master Mechanical Engineering

Master Thesis
[40EC]
Course code: 191199198

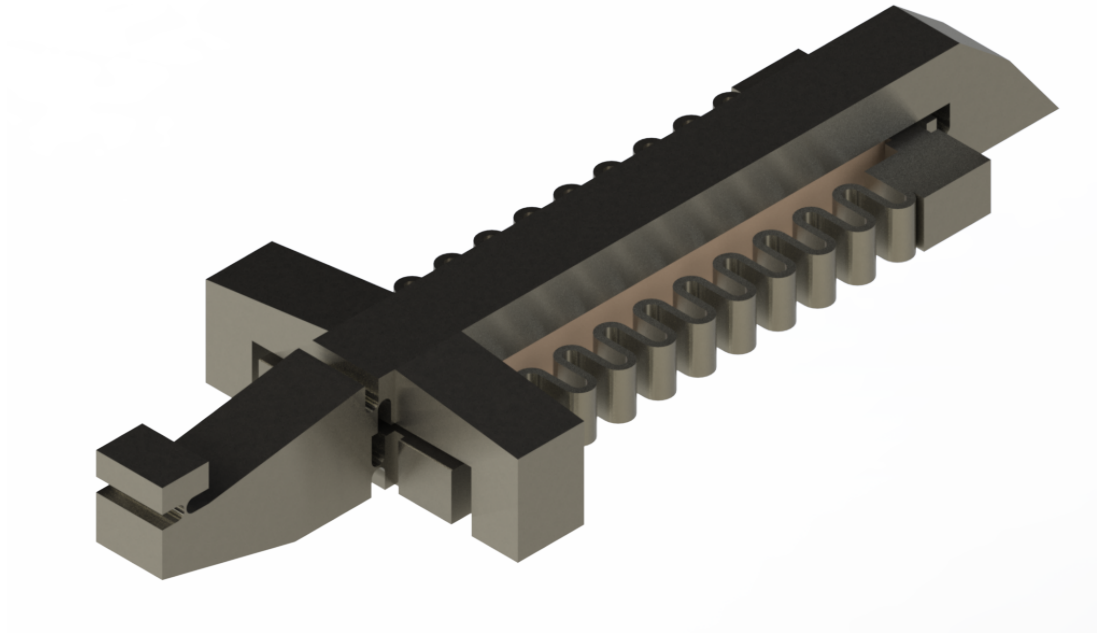

Author
C.C.J. Hollaar

Supervisor
Dr.Ir. A.P. Berkhoff

Chair
Prof.Dr.Ir. D.M. Brouwer EngD

CONFIDENTIAL

June 30, 2023

ABSTRACT

In the past, designs have been proposed for making energy-efficient thin flat acoustic sources. These designs relied on piezoelectric stack actuators placed parallel to the diaphragm and a conversion mechanism that moved the diaphragm, which consisted of a lightweight sandwich structure. These past designs were only usable for limited frequency ranges and contained over- and underconstraints.

In this master thesis a simpler design was made and modelled. Based on modelling results the design was optimised through multiple iterations. Improvements were aimed at increasing the first natural frequency of the system whilst not exceeding the stress fatigue limit. Once sufficient simulated performance was achieved, the design was manufactured to validate the model. Due to practical constraints the manufactured design deviates from the optimised model in multiple ways. In order to validate the model using the manufactured design, the model was adapted to the manufactured specs.

The manufactured design was tested to identify the natural frequencies and subsequently the acoustic behaviour was tested using microphones. The results showed a natural frequency of 340Hz, which was predicted quite well by the model. Using this model a thin sound source for 20-500Hz seems achievable.

CONTENTS

Abstract **1**

Summary **5**

1 Introduction **6**
1.1 Motivation . . . 6
1.2 Research objective . . . 6
1.3 Research assignment . . . 7
1.4 Readers manual . . . 7

2 Literature study and patent research **9**
2.1 Types of acoustic sources . . . 9
2.1.1 Patents around flat acoustic sources . . . 9
2.2 Noise cancelling . . . 11
2.2.1 Passive noise cancelling . . . 11
2.2.2 Active noise cancelling . . . 12
2.3 Piezo-electric actuation . . . 13
2.3.1 Piezoelectricity . . . 13
2.3.2 Piezoelectric transducers . . . 13
2.4 Flexure Hinges . . . 14
2.4.1 Types of flexure hinges . . . 15
2.4.2 Benefits of flexure hinges . . . 15
2.4.3 Notch hinges . . . 15
2.5 Flexure motion conversion . . . 15
2.6 Patents around flexure motion conversion . . . 16
2.7 Patents around perforated honeycomb sandwich plates . . . 16

3 Design requirements **19**
3.1 Natural frequencies . . . 19
3.2 Thickness of the sound source . . . 19
3.3 Durability . . . 19
3.4 Energy efficiency . . . 19
3.5 Displacement . . . 19
3.6 Complexity . . . 20
3.7 Innovativeness . . . 20

4 Initial Design decisions **21**
4.1 Principal Design . . . 21
4.2 Converter . . . 21
4.2.1 Piezoelectric stack actuator . . . 21
4.2.2 Hinges . . . 22
4.2.3 Connector . . . 23

4.2.4 Frame . . . 23
4.2.5 Converter height and depth . . . 23
4.2.6 Material selection . . . 23
4.2.7 Production method . . . 24
4.2.8 Schematic . . . 24
4.3 Sandwich plate . . . 26
4.3.1 Shape . . . 26
4.3.2 Sandwich structure . . . 26
4.3.3 Equivalent plate . . . 26
4.4 Box . . . 28
4.4.1 Walls . . . 28
4.4.2 Rubber strips . . . 28

5 Design iterations **30**
5.1 Initial simulation design . . . 30
5.1.1 Results and conclusions . . . 31
5.2 Improvements . . . 31
5.2.1 Frame . . . 31
5.2.2 Connector . . . 32
5.2.3 Prestress mechanism . . . 33
5.2.4 Hinges . . . 35
5.2.5 Piezo . . . 38
5.2.6 Sandwich plate . . . 38
5.2.7 Stiffness of air in cavity . . . 38
5.3 Sandwich plate improvement . . . 39
5.3.1 Different equivalent plate . . . 39
5.3.2 Local stiffening . . . 41
5.3.3 Increasing plate thickness . . . 42
5.3.4 Core fraction optimisation . . . 42
5.3.5 Weight reduction . . . 43
5.4 Final design . . . 45

6 Acoustics **47**
6.1 Acoustic modelling . . . 47
6.2 Acoustic validation . . . 49

7 Manufacturing **50**
7.1 Piezo . . . 50
7.2 Sandwich plate . . . 50
7.3 EDM parts . . . 51
7.4 Supports . . . 52
7.5 Box . . . 52
7.6 Amplifier . . . 52
7.7 Assembly . . . 52

8 Validation **54**
8.1 Displacement . . . 54
8.2 Natural frequencies . . . 54
8.3 Acoustic behaviour . . . 57
8.4 Laser Vibrometer . . . 57
8.5 Results . . . 57
8.5.1 Determining natural modes and frequencies . . . 57

8.5.2 Noise 58
8.5.3 Determining the acoustic behaviour 59

9 Conclusions and Recommendations **61**
9.1 Conclusions 61
9.2 Recommendations 61

References **63**

A Appendices **66**

B Types of acoustic sources **69**
B.1 Dynamic loudspeaker 69
B.2 Piezo speaker 69
B.3 Electrostatic 70
B.4 Distributed mode loudspeaker (DML) 70
B.5 Alternatives 72

SUMMARY

In the past, designs have been proposed for energy-efficient thin flat acoustic sources. These designs relied on piezoelectric stack actuators placed parallel to the diaphragm and a conversion mechanism that moved the diaphragm. This diaphragm consisted of a lightweight sandwich structure. In practice, the designs turned out to have a very limited frequency range for operating and because of their complexity these designs were error-prone. Also, the Degrees of Freedom were not exactly constraint, resulting in undesirable motion.

In this master thesis a simpler design was made and modelled in COMSOL Multiphysics. Based on modelling results the design was optimised through multiple iterations. Improvements were aimed at increasing the first natural frequency of the system whilst not exceeding the stress fatigue limit.

Once sufficient simulated performance was achieved, the design was manufactured to validate the model. Due to practical constraints such as time, availability and budget, the manufactured design deviates from the optimised model in multiple ways. In order to validate the model using the manufactured design, the model was adapted to the manufactured specs. Due to some connection failures in the assembly and time constraints improvisational deviations from the design were performed.

The manufactured design was tested to identify the natural frequencies and subsequently the acoustic behaviour was tested using microphones. The first natural frequency of the source was found to be 340Hz whereas 390Hz was predicted. This is likely due to a combination of manufacturing inaccuracies, improvisation and some effects not being taken into account in the model.

As the behaviour of the manufactured prototype was predicted reasonably well by the model, it can be expected that the optimised model would also work quite well, making a thin speaker for 20-500Hz achievable.

1 INTRODUCTION

1.1 Motivation

The maximum thickness of a sound source can in some cases be limited by spatial or aesthetic constraints. A smaller source however usually also means lower sound pressure and/or lower efficiency. If the sound source could be made thinner without a large loss in sound production and efficiency, this could fill the gap. This type of sound source could especially be useful in the area of active noise cancelling, as space around noise generating sources is often very limited. An example is in ventilation ducts, where the humming sound of ventilators is carried through entire buildings. Another place where this could be beneficial is in an anechoic chamber, where the cancelling of noise is very important and space is often limited.

In the past research around designing a thin, flat sound source has been conducted. This has amongst other things resulted in (manufactured) designs like [1] and [16]. In these designs a sandwich plate with a perforated bottom plate is used to increase the efficiency of the mechanism. In order to make the mechanism even thinner, a design was made in which the actuator was placed parallel to the moving diaphragm instead of in line with it, using a piezoelectric stack actuator and a flexure mechanism to change the direction of the motion, as visible in figure 1.1 [34]. This principle has been shown to work as a way to reduce the thickness, though it can be improved upon significantly. One of the problems with the design is that the motion converter was not exactly constraint, as the centre body and the attached bodies on both sides are attached to the other bodies by a parallel flexure-like mechanism, allowing for unconstrained left-right translation of the centre body. Another problem identified was the relatively low first natural frequency, which led to a small bandwidth. The modelled and experimental results of this design can be viewed in figure 1.2.

1.2 Research objective

The objective of the present assignment is to design, manufacture and test an improved version of the displacement converter. The first natural frequency of the system should be higher

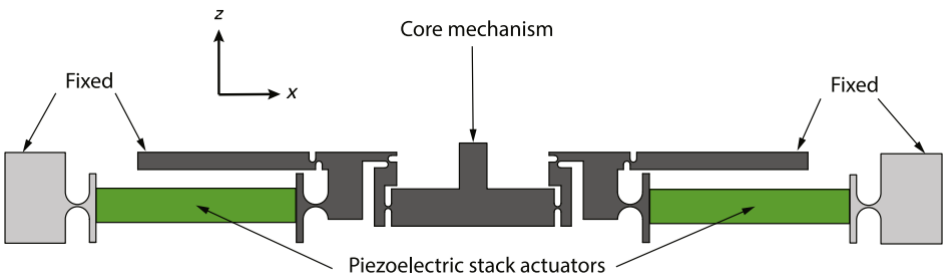

Figure 1.1: The conversion mechanism that is to be improved upon, as designed by [34].

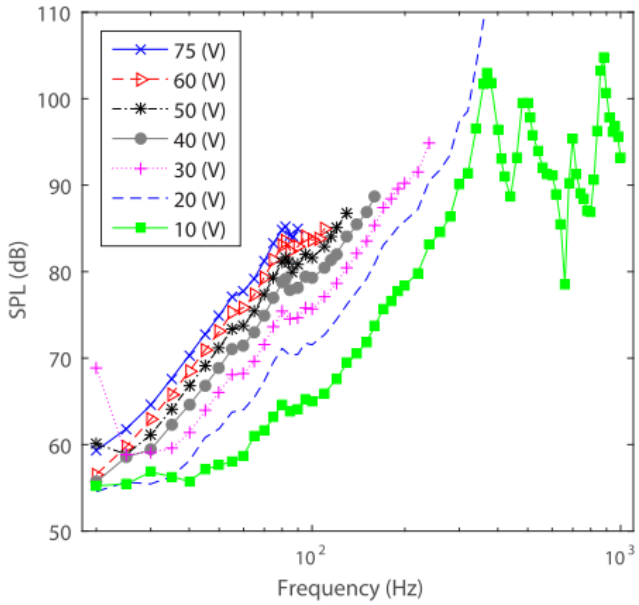

Figure 1.2: Frequency-Sound Pressure Level graph, measured directly in front of the sound source for various voltages, taken from [33]. First natural frequency occurs around 370Hz.

than 370Hz, which was found in previous works, thereby increasing the bandwidth. The design should also be better constrained and less complex. Subsequently, the displacement converter is tested in combination with a prestressed piezoelectric actuator and the acoustic source. Finally, the acoustic properties of the acoustic source are evaluated, such as the frequency response and the achievable sound pressure levels.

1.3 Research assignment

The problem and research objective are translated to the following research assignment:

"Modelling and improved design of a displacement converter for a thin sound source"

1.4 Readers manual

Following this introduction, the report continues in chapter 2 with a literature study, exploring the theory around relevant concepts for the assignment and a patent study in which similar patents are discussed in order to make sure that the assignment is not unintentionally plagiarising existing work. In chapter 3 the assignment is combined with relevant theory to make a list of requirements for the design that is to be made. In chapter 4 a basic design is discussed with relevant decisions and assumptions, it subsequently consists of an elaboration on the iterative design process which results in a final design. Chapter 6 discusses the acoustics of the design and the way it is modelled to predict the behaviour of the designed acoustic source.

Up to and including chapter 6 the aim was to make an optimal design, using theory and models to iterative improve the acoustic source and to predict its behaviour. Chapter 7 is where reality comes in and the optimised design has to be realised as closely as possible while staying within timely and budgetary constraints. Chapter 8 explains how the realised mechanism

is used to validate the digital model and shows the results of this validation. In chapter 9 relevant conclusions are drawn and recommendations are made regarding both improvements on the discussed design (process) and future research surrounding this topic. Lastly, relevant appendices can be found at the end of the report.

2 LITERATURE STUDY AND PATENT RESEARCH

In this chapter relevant theoretical concepts around the design assignment are explored in order to learn more about what has already been done and find out what elements could be used in this design.

A patent study was also conducted to prevent accidental plagiarism and make sure that the design made is innovative. Espacenet was used to identify patents similar to the design assignment. These patents are shown near the relevant concepts. The search terms used for each section are shown in the respective sections. European patents are valid for at most 20 years [24]. Whether a patent is (still) valid within the 20 year period depends on multiple factors, among which whether the owner has paid the annual fees. For most patents this is not visible on Espacenet.

2.1 Types of acoustic sources

To determine whether other types of acoustic sources could be used to make a better design, some research was conducted into this direction. As the assignment explicitly stated the type of source to be used, this section was deemed not relevant enough and was therefore moved to the appendix.

2.1.1 Patents around flat acoustic sources

The flat sound source design which is to be improved upon is based on patent [1]. This is for ”A sound generator, particularly a loudspeaker, configured to emit sound, comprising a rigid element (2) enclosing a plurality of air compartments (3), wherein the rigid element (2) has a back side (B) comprising apertures (4), and a front side (F) that is closed, wherein the generator is provided with at least one actuator (6), for instance one or more electromagnetic actuators and/or piezoelectric elements, configured to actuate the rigid element (2) for the generation of the sound.” [1], visible in figure 2.1

Besides this, a search was conducted using different combinations of the following search words: ”flat, thin, small thickness, flat-panel, acoustic, sound, source, generator, speaker, loudspeaker, box”. The search was limited to acoustic sources with a moving membrane/plate, as electrostatic loudspeakers are also flat, but very different in working principles.

An early flat sound source was [21] from 1967. This sound source uses a flat membrane, driven by a VCM. The membrane is bent by the VCM, which sticks out to the back in the centre of the source, as visible in figure 2.2.

Another flat sound source patent was found for [25]. This is a patent for an elliptical flat sound source driven by a Voice Coil Plate. A rigid plate is actuated to generate sound. A picture of

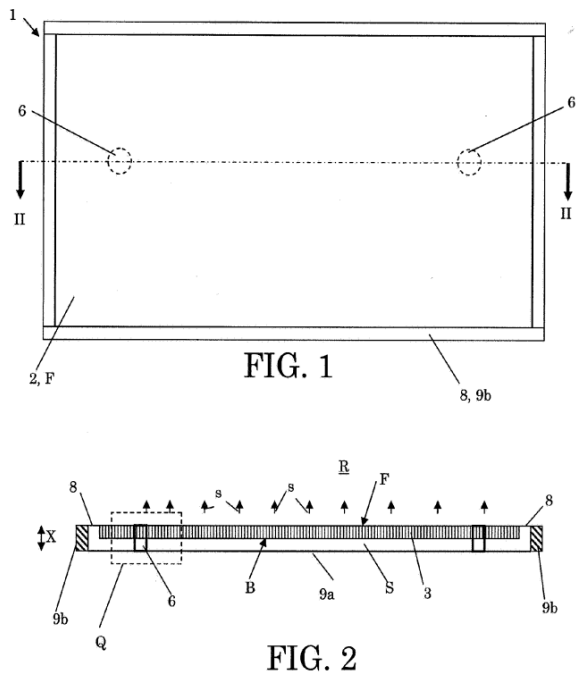

FIG. 1

FIG. 2

Figure 2.1: Figure showing the configuration of the flat sound source of [1]. Fig.1 is the top view, Fig.2 is a section view at II-II in Fig.1

the patented source is visible in figure 2.3.

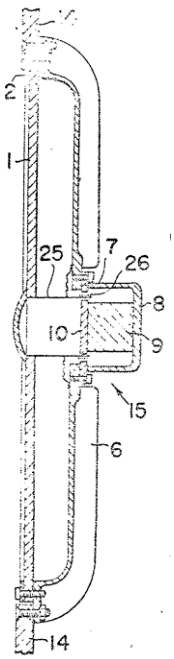

Figure 2.2: Figure showing the configuration of the flat sound source driven by a VCM of [21]

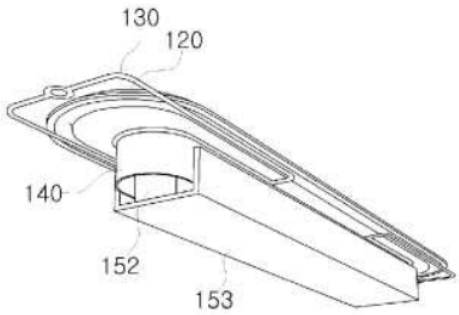

Figure 2.3: Figure showing the configuration of the flat sound source driven by a VCM of [25]

Another patent for a flat sound source also utilises a sandwich panel consisting of two aluminium face plates separated by an aluminium honeycomb structure. This does however not have per-

forations in the back plate. This design has a piezoelectric transducer inside one of the cells of the honeycomb structure to produce the higher frequencies [19]. The patented design is visible in figure 2.4.

More flat-panel sound source patents were identified in [10], visible in figure 2.5. This source consists of a flat plate supported and sealed at the edges to create en enclosed box of air. The plate is excited in the centre. The source can be designed for utility within a certain frequency range. Outside this range phase modulation occurs, which interferes with the quality of the sound [10].

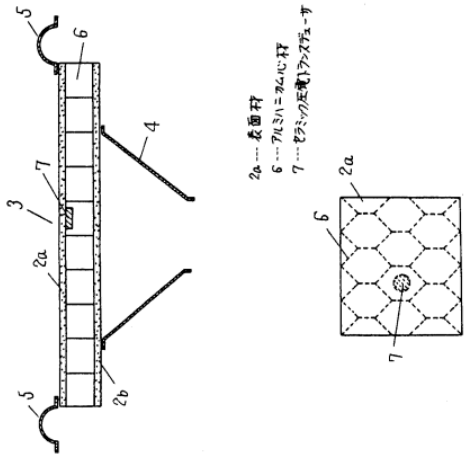

Figure 2.4: Figure showing the flat sound source with honeycomb sandwich plate of [19]

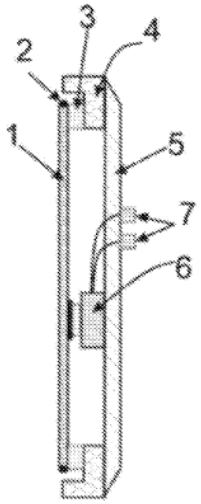

Figure 2.5: Figure showing the configuration of the flat-panel sound source of [10]

Multiple small circular flat-panel VCM driven loudspeakers have been patented both with rigid and non-rigid diaphragms. Some examples of these are [42] and [41], visible in figures 2.6 and 2.7 respectively. There are many more examples of these, but as both their driving mechanism and their sound generating membrane are not similar to this assignment, no more are included.

Some more patents were found which might be relatable, but as no translation, drawings or information on the status of these patents were available and only a very short description in English was available, no conclusion could be drawn on these and therefore these were omitted in this study. The search terms resulted in a total of around 500 patents, of which around 15 were somewhat relevant to this project.

2.2 Noise cancelling

A growing area of interest is noise cancelling, the ability to prevent sound from propagating. This has been done for a long time through passive means, but there are also active means to do this.

2.2.1 Passive noise cancelling

Passive noise cancelling encompasses all ways to block sound physically. This can be done through reflection, deflection and absorption. For reflecting sound, a high impedance bound-

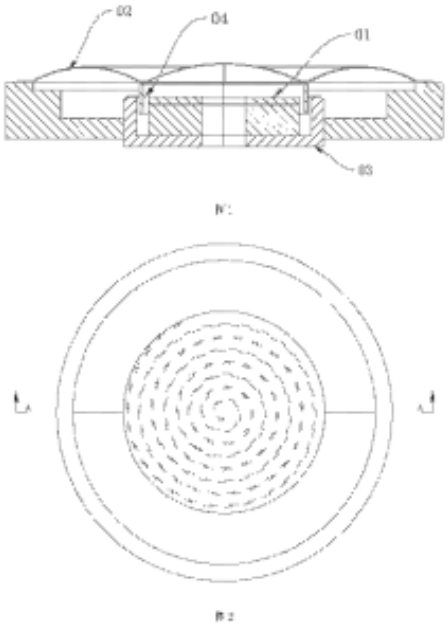

Figure 2.6: Figure showing the flat circular VCM driven sound source of [42]

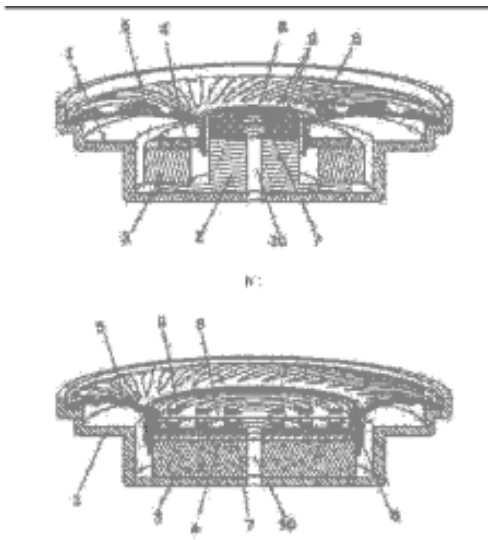

Figure 2.7: Figure showing the flat circular VCM driven sound source of [41]

ary is needed. Often this means a rigid wall of some sorts. Other ways of reducing the sound transmitted are changes in cross-sectional area. That means that when sound is transmitted from a small room through a wide room towards another small room, there are two impedance boundaries at which a significant portion of the sound energy is reflected instead of transmitted [2]. Other ways to cancel out noise is by using acoustic foam. This is wavy or spiky foam material with damping properties, often seen in music studios. These foams are most effective at damping higher frequencies, as visible in figure 2.8. For the lower frequency range, the acoustic foam spikes have to be very large, and therefore take up a lot of room.

Another option is to use resonators like a quarter wavelength resonator or a Helmholtz resonator. These resonators are tuned to a specific frequency, which is dampened. This can be very effective and is for instance used in car exhausts. Outside the tuning frequency the resonators do not interfere with the noise.[2].

2.2.2 Active noise cancelling

Another way to cancel out noise is through active noise cancelling (ANC). ANC at least consists of the following components: a microphone to measure the incoming noise, a controller to process this noise and generate a an opposite signal and a loudspeaker to emit the opposite signal [13]. By sending out the exact opposite sound signal to the noise, the noise can no longer continue.

An ANC system is limited by the quality of the microphone and the quality of the loudspeaker and on its own never completely cancels out the noise, but a very large portion of the sound can be negated through this. The frequency range for which ANC can be used is only limited by the frequency ranges of the loudspeaker and microphones, which could in theory be the entire audible range. [13].

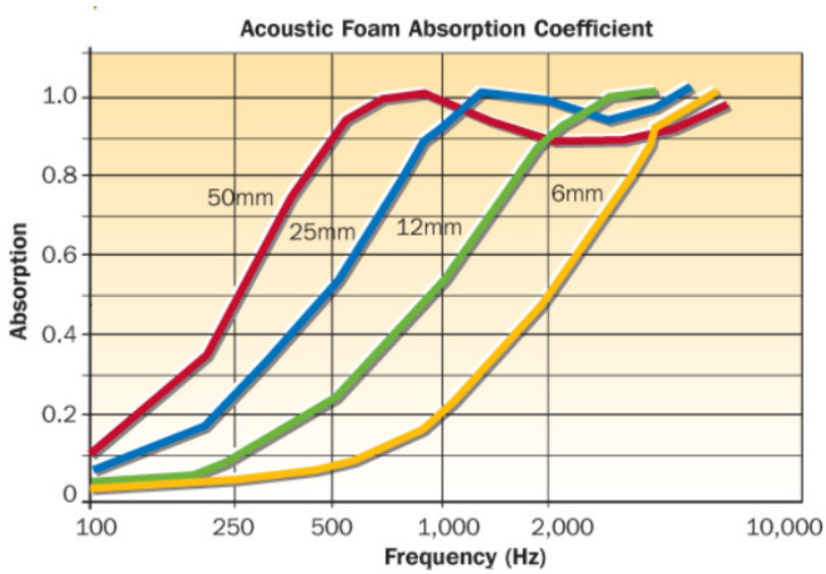

Figure 2.8: Absorption coefficients of different sizes of acoustic foam. Larger spikes have better absorption at lower frequencies [20].

2.3 Piezo-electric actuation

As the system to be designed is to be driven by a piezoelectric stack actuator. For better understanding, more insight in this type of actuator is needed.

2.3.1 Piezoelectricity

A piezoelectric material is a material that develops a charge on its surface when stress is exerted on it. Naturally occuring materials with this property are quartz and tourmaline, though many artificial materials have been made with this property as well. The property also works in the other direction: when a piece of piezoelectric material is charged, a strain is induced in it[23].

When crystals are randomly oriented, this property is not very useful, but when the crystals are aligned, it becomes useful. The aligning of these crystals is called polling. During this process a very strong DC field is applied to the material, which causes small crystals to orient themselves in the direction of the field. Once the DC field is removed, the crystals will only reorient themselves slightly [23].
Piezoelectric materials can be used on two ways. By measuring the charge that is generated under stress, the stress that causes it can be calculated. Therefore it can be used in pressure sensors. The other way to use it is by applying a charge on it, which causes the material to strain. Though this strain is relatively small compared tot the size of the material, the material can exert a lot of force under the charge. This straining can be used for many applications [15].

2.3.2 Piezoelectric transducers

Piezoelectric materials can be used a transducer. Under charge, the material changes shape. It elongates in one direction, while it shortens in the other directions. Though this elongation is only small compared to the size of the material, it can be used when precision is needed. Using these types of transducers, sub-micron level accuracy can be achieved. The material

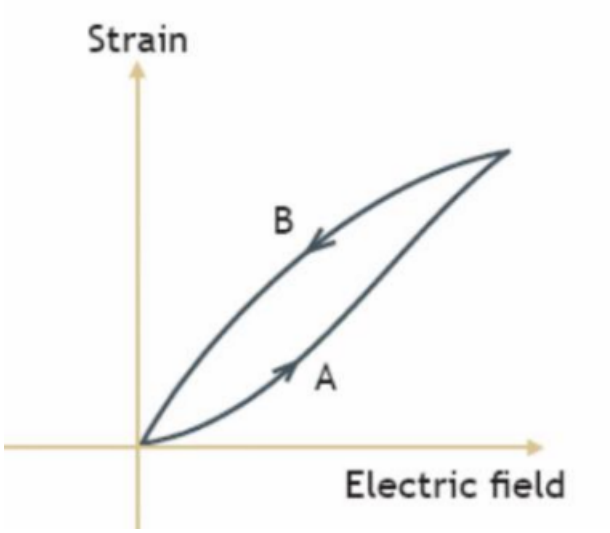

Figure 2.9: ”Hysteresis” is when the strain at a given charge is dependent on whether it is being charged or discharged [23].

also reacts fast to changes in charge [15].

An important factor in piezoelectric materials is hysteresis. This is the path dependency of the strain. When applying the charge, the material will strain differently from when unloading it, which means that for a given charge between 0 and the maximum charge, it is not unambiguous what the corresponding strain is. This is pictured in figure 2.9.

As the material only strains relatively little compared to its size, large displacement requires large pieces of material. Due to manufacturing constraints, the sizes at which piezoelectric material can feasibly be produced are very limited [15]. In practise this is circumvented by stacking multiple piezo elements on top of each other. This way larger displacements are possible, though still not large in comparison to other types of actuators. This type of actuator is called a piezoelectric stack actuator. Displacements that are achieved with this kind of actuator are in the order of a thousandth of the length of the actuator [23].

These types of actuators are very delicate. Piezoelectric material is usually very brittle and can only deal with compressive stresses. When designing a mechanism in which a piezoelectric actuator is placed, special care needs to be taken not to put any radial forces, tensile forces, bending or torsion on the piezo. In order to prevent tensile forces two options are often used: only use a positive charge during operation or use a pretension mechanism. The first option is most applicable during (quasi-)static operation; the second during dynamic operation [22]. The pretension mechanism is a mechanism that usually consists of multiple very stiff springs that are initially smaller than the actuator. These are extended and placed around the actuator. The springs will try to go back to their relaxed position, clamping the actuator and exerting a compressive force on it. If well designed, tensile forces will never exceed the compressive forces of the pretension mechanism, which prevents tensile forces on the actuator [22].

2.4 Flexure Hinges

The design is to be made using flexure hinges. Where conventional hinges consist of multiple parts sliding through or over each other, flexure hinges consist of a single part which deforms elastically to provide a rotation.

2.4.1 Types of flexure hinges

There are multiple ways for elastic elements to create a hinge function. These element come down to variations of the hinges in figures 2.10, 2.11, 2.12, 2.13, 2.14 and 2.15. All of these provide rotations in one direction, except for the toroidal hinge in figure 2.12, which is essentially a combination of 2 notch hinges [28].

2.4.2 Benefits of flexure hinges

In comparison to conventional hinges flexure hinges have multiple benefits. As there are no elements sliding over each other, there is no play. This means that a position can be completely determined which is very desirable in high precision areas. Another benefit of flexure hinges is that no internal friction occurs. This reduces wear significantly, which increases the lifespan and it removes the need of lubrication, which removes the need for maintenance [28].

2.4.3 Notch hinges

Most of these flexure hinges either require multiple parts joined together or require complex machining to manufacture. This is not true for the notch hinges, which only require the removal of some material. These types of hinges are well documented and have been studied extensively. Depending on desired stiffness and compliance, an optimal notch hinge can be designed through calculations like in [28]. These equations have been practically validated in studies like [38].

2.5 Flexure motion conversion

Using and combining multiple flexible elements, a mechanism can be designed to convert the movement of an actuator to the movement of another body. For this assignment the conversion of interest is the conversion of the linear horizontal motion of an actuator to a perpendicular vertical motion of a diaphragm. The mechanism to be designed should therefore have 1 degree of freedom (DOF). If the designed mechanism is 2-dimensional, the degrees of freedom can be calculated through the following equation:

$$n_{DOF} = 3 \times n_b - n_c - n_d \tag{2.1}$$

in which n_{DOF} is the number of degrees of freedom, n_b is the number of bodies in the mechanism and n_c is the number of constraints and n_d is the number of driven translations and rotations. Each unconstrained body has 3 degrees of freedom: 1 rotation (around the z-axis) and 2 translations (in the x- and y-direction). A rotational hinge constrains 2 translational DOF's. It is very important to take care when calculating the degrees of freedom using this equation, as this does not take into account multiple constraints of the same DOF. This means that a mechanism can be both over and underconstrained at the same time, while equation 2.1 shows no DOF's should be present. Therefore this equation is only indicative. If this equations is nonzero, the system cannot be exactly constrained, while if it is zero, further examination is required.
The mechanism in figure 1.1 for instance consists of 7 bodies and 10 rotation hinges. If all bodies are considered rigid, equation 2.1 yields $7 \times 3 - 10 \times 2 - 2 = -1$ DOF. This means that the system should be overconstrained by 1. Overconstraints can result in very high stresses and are therefore undesirable. Further examining the system actually gives a different result. As told in the previous chapter, the left-right translation of the centre bodies is unconstrained, and therefore there are even more overcontraints as well.

Other mechanisms to convert a horizontal motion to a vertical motion are also possible. Some options are shown in figures 2.16 and 2.17. The first one is quite complex as it requires 4 actuators to work in sync to work properly. The second is less complex but is relatively thick in the driving direction.

Another option is to use a rotating intermediary body, like in the figure below:
In order to analyse this mechanism, it is split in two parts. The horizontal plate that is suspended by springs is considered separate from the mechanism below it. Following equation 2.1, the lower mechanism has 2 bodies, 3 rotational hinges. This results in 0 DOF's, an exactly constraint system. Further examination shows that this is correct: for each length of the actuator on the lower left, the centre body is pivoted around the hinge connected to the ”fixed world”. For small displacements, this yields a near-pure vertical displacement of the hinge connected to the horizontal plate. If the plate would be rigidly connected to the mechanism underneath it, the very small rotation of the centre body would result in very small rotation of the plate, which would be amplified by its length. The hinge in between negates this rotation and the plate is guided by the springs.

As this system only has parts next to and above the actuator, it can potentially be made quite thin. For large strokes, a parasitic sideways motion of the moving plate would occur, but with small strokes this motion is very small.

2.6 Patents around flexure motion conversion

Similar to before, a study is conducted into motion converters that use flexures. Search words that have been used in various combinations on Espacenet are: ”Flexure, flexures, flexible element, flexure hinges, notch hinges, motion converter, motion conversion, direction changer”.

Many patents showed up in the search, but after closer examination, none were deemed relevant to this assignment. This is most likely because it is a hard topic to get a patent in, as these mechanisms are often already in use in many other fields and therefore not unique enough.

2.7 Patents around perforated honeycomb sandwich plates

The last category of patents to be studied is the area of perforated sandwich plates for sound generation. Besides patent [1], similar patents are sought through Espacenet. Search words include combinations of the following: ”Perforated, hexagonal, honeycomb, sandwich plate, panel”.

Honeycomb structured sandwich panels are often used for their sound isolation properties, as they are lightweight. This property is used in patents like [7], [40], [39] and [30] amongst many others.

For sound generation the sandwich plates are used amongst others in patent [19]. These make use of the fact that the sandwich plate is lightweight, relatively stiff and flat.

None were found however that also use the sandwich plate in some way or another to increase the effective air volume of the enclosure. In doing so, the force required to move the plate is reduced in comparison to a solid plate, thereby reducing the energy required to achieve a certain displacement, i.e. the efficiency is increased. [33].

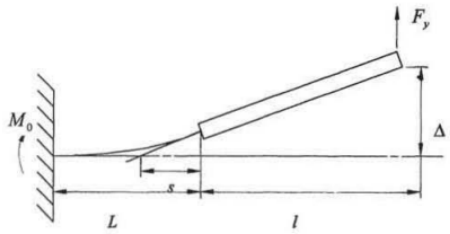

Figure 2.10: Cantilever flexure hinge [28]

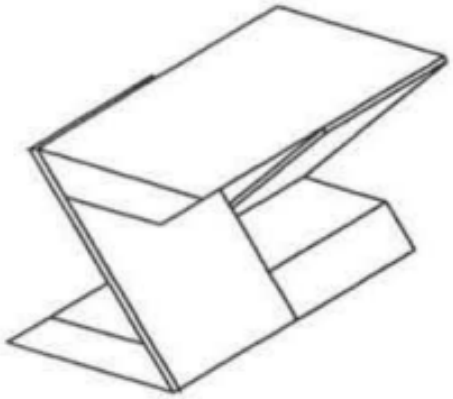

Figure 2.11: Cross-strip pivot hinge [28]

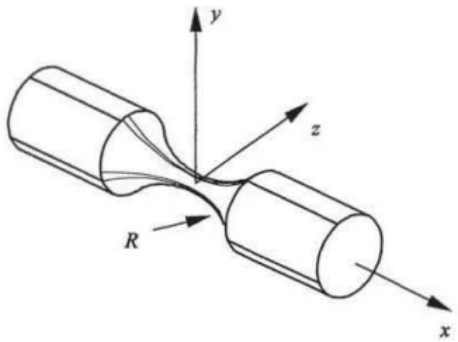

Figure 2.12: Toroidal hinge [28]

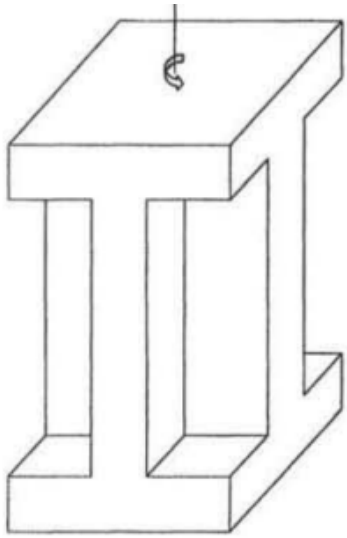

Figure 2.13: Cruciform hinge [28]

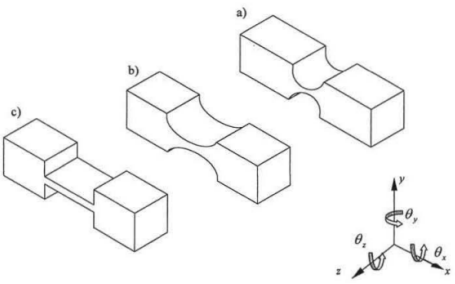

Figure 2.14: Three types of notch hinges [28]

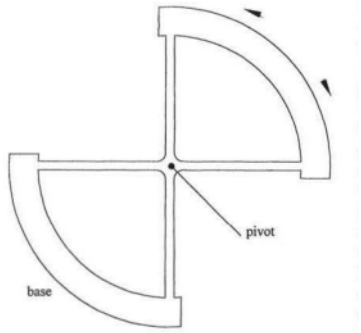

Figure 2.15: Cartwheel flexure [28]

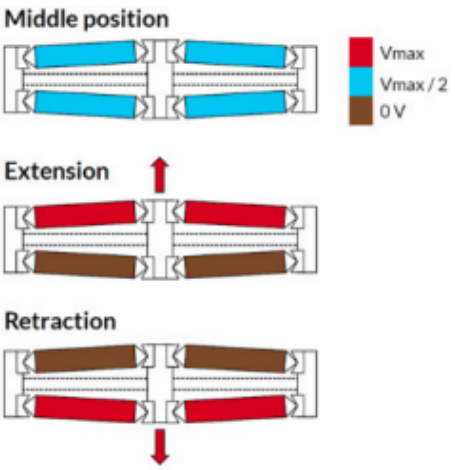

Figure 2.16: Mechanism with 4 actuators to create out-of-plane motion [27]

Figure 2.17: Mechanism using 1 actuator to create out-of-plane motion [8]

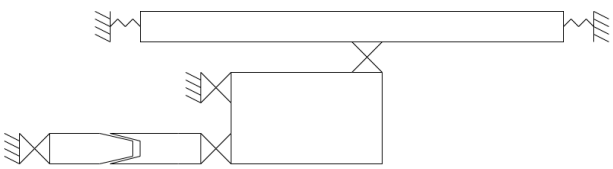

Figure 2.18: Flexure motion converter with rotating intermediary body

3 DESIGN REQUIREMENTS

In this chapter the aim of this research is translated to design requirements. As the goal is to improve on the designs in [34], [35] and [33], visible in figure 1.1, most requirements follow from the performance found in those papers and in the research assignment.

3.1 Natural frequencies

From ref [33] it can be found that the first natural frequency of the design which is to be improved on occurs around 370 Hz, as shown in figure 1.2. As the first natural frequency of the design determines the range in which the sound source is usable, this frequency needs to be increased significantly.

The assignment giver has set a first natural frequency of over 1000Hz to be desirable. A first natural frequency of over 500Hz is deemed to likely be at least achievable by the assignment giver.

3.2 Thickness of the sound source

One of the unique selling points of this type of sound source is that it is much thinner than its VCM counterparts. Therefore the total thickness of the design should not exceed 50mm.

3.3 Durability

The sound source should not require any maintenance during its life cycle. It must operate constantly for at least 10 years. This means the design must not have moving parts that are subject to friction, which results in the use of flexures. As these flexures have to operate continuously for 10 years at an average of 500Hz, the hinges have to withstand over 10^{11} operating cycles. The material and loads have to be chosen accordingly.

3.4 Energy efficiency

Though not explicitly stated in the assignment, one of the benefits of the previous design that has to be kept is the fact that it is more energy efficient than its conventional counterpart. This is achieved because of the combined use of the piezoelectric stack actuator and a class-D amplifier [35]. Because of this, a piezoelectric stack actuator has to be used in the design.

3.5 Displacement

In order for the sound source to be useful, it has to produce enough sound. While it is hard to determine exactly how much is needed, a plate displacement of at least 100μm is deemed necessary.

3.6 Complexity

The motion conversion mechanism in the previous designs is quite complex and because of that it is more prone to errors due to miss-alignment when assembling and production errors in the parts. It is therefore desirable to reduce the complexity of the design.

3.7 Innovativeness

The design has to be innovative in that it cannot copy something that has already been made. It is possible to combine elements of existing solutions as long as it is in a unique way. In order to make sure this condition is satisfied, the patent study in the previous chapter has been conducted.

4 INITIAL DESIGN DECISIONS

In this chapter important design decisions are substantiated. This is for parts, subparts and for the design as a whole. The design is divided in the parts converter, sandwich plate and box. In the next chapter these decisions are used to make a model upon which design iterations are made.

4.1 Principal Design

For the principal design, several decisions have been combined to reach the design in figure 2.18. In order to reduce complexity it was decided that the design should contain as few elements as possible. Designs with multiple actuators were therefore put aside. The simplest way to change the direction of motion is using an elbow mechanism. This consists of a rotational hinge and two perpendicular arms connected rigidly to each other in the pivot point. The other elements follow from design principles for piezoelectric actuators and the fact that the diaphragm should only move vertically. All elements are further elaborated on in this chapter.

4.2 Converter

The converter is the part that is responsible for generating the motion of the sandwich plate. This part consists of a piezoelectric stack actuator, four notch hinges, a connector which connector the parts together and a frame which acts as the ”fixed world”.

4.2.1 Piezoelectric stack actuator

As one of the requirements is to use a piezoelectric stack actuator, this is chosen for actuation of the system. Properties that have to be decided are the dimensions, the stroke, the blocking force,the method of pretension and the connection to the system.

A piezoelectric stack actuator, piezo in short, is strong in handling compressive forces. The piezo however is very brittle and therefore cannot handle tensile forces, lateral forces and torque

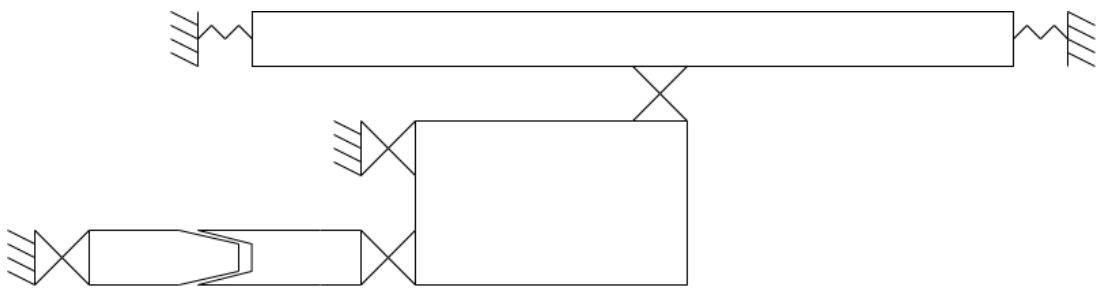

Figure 4.1: The chosen base design

[4]. Therefore all of these have to be prevented.

As the piezo is used as actuator and thus extends and shrinks, reversing the direction of the plate causes tensile forces on the piezo during shrinking. In order to prevent the piezo from breaking, a preload is added to the piezo in order to overcome these tensile forces. This can be done according to the principles in [6].

In order to prevent lateral forces, the piezo can only be loaded its length direction. As the chosen design will have (slight) parasitic motion in the lateral direction at the end of the piezo, a mechanism is required to absorb these forces. This can be done by using the techniques shown in figure 52 in [4].

Lastly, torsion has to be prevented from affecting the piezo. Using the techniques shown in figure 52 and 53 of [4] will do this. Torsion in the system is not only undesirable in the piezo, but also in other parts and therefore it is even better to prevent it as a whole. This can be done by precise manufacturing and symmetric actuation.

In conclusion a preload is to be designed for the piezo and a mechanism is to be designed to absorb the lateral forces caused by parasitic motion of the system. It is possible to buy piezos with preloads already attached, but these are usually situated around the piezo in all directions, causing to thickness of the entire mechanism to increase. To prevent this, a preload was designed that does not cause the sound source to increase in thickness. This was achieved by placing the spring elements to the sides of the piezo, as visible in figure 4.2.

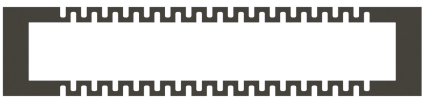

Figure 4.2: Preload mechanism designed to prevent tensile forces, lateral forces and torsion on the piezo. This design specifically was made to not increase the thickness of the sound source.

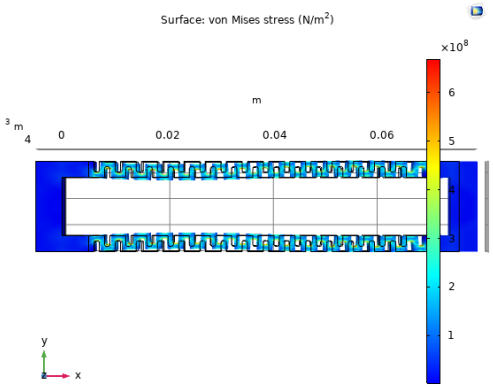

Figure 4.3: Stresses in the preload mechanism in maximum excited position.

4.2.2 Hinges

The chosen design relies on rotational hinges. As the requirements state that the design has to be maintenance free, these hinges should be frictionless. Therefore the hinges are chosen to be flexure hinges [28].

As reducing complexity is one of the goals of the assignment, keeping the number of parts to a minimum is desirable. As shown in the literature study, notch hinges are best suited in this regard and are therefore chosen.

In this mechanism, the hinges should all be very compliant for rotation while remaining stiff enough for translation and undesired rotations. For different types of notch hinges, the compliance and stiffness has been tested in [38]. From this research it is clear that elliptical and circular notch hinges provide the best rotational compliance while hyperbolic notch hinges provide the best translational stiffness. As more rotational compliance corresponds to lower actuation forces and lower stresses in the hinges, this is desirable. Because the hinges still need to be stiff in the translational direction, initially circular notches are chosen, because these perform better in this regard [38].

4.2.3 Connector

The hinges have to be connected to a rigid part in the way that is shown in figure 4.6. This part from now on is called the connector. The connector has to convert the horizontal movement generated by the piezo into a vertical movement which is followed by the plate. It has to deform as little as possible while doing this.

4.2.4 Frame

A frame is required to connect the converter to the ”fixed world”. This connection is to be made at the hinges on the left side of figure 4.6. In the initial design, the frame is left out as its influence is estimated to be low. In later stages it will be added.

4.2.5 Converter height and depth

The converter has to be as thin as possible while retaining enough stiffness and displacement. Enough space is required for the hinges and for the piezo and for the lever to work, also some height is required. The depth of the converter is less crucial. It should be large enough to be stiff enough, which should be easy as there is no actuation in that direction. More depth also means more weight. As the weight of the moving parts has to be moved by the actuator, lower weight means higher efficiency. Lastly the depth is also dependent on available material thickness. An initial choice is made for 10mm. The influence of the thickness will be evaluated later in this report.

4.2.6 Material selection

The converter has to operate without maintenance for very many cycles, therefore the material has to be selected carefully. The selection criterion’s are:

- High fatigue strength (needs to withstand over 10^{11} cycles)
- Low density (mass negatively affects energy-efficiency and natural frequencies)
- Sufficient stiffness (should only deform due to the piezo)
- EDM machinable (very high precision is required)

Fatigue strength

In technical data sheets (TDS) the fatigue strength is usually given for 10^6 or 10^7 cycles. This is maximum stress during an operation cycle for which it takes that amount of cycles for the specimen to break. As the amount of cycles required for this product far exceed this amount of

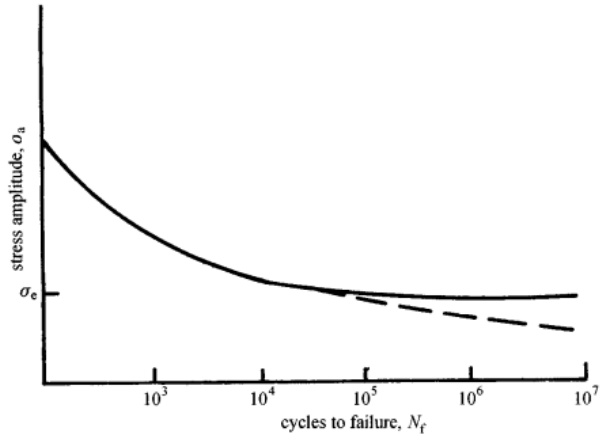

Figure 4.4: S-N graph showing the amount of cycles to breaking for increasing stress levels for most steels (solid line) and for other alloys (dotted line). The solid line does not decrease after 10^6 cycles, which shows that for stresses under that level cycles can be repeated indefinitely without breaking.[31]

cycles, this fatigue strength does not suffice. Behaviour beyond this amount of cycles is dependent on the type of material.

For steels under constant amplitude loading conditions, there is a plateau in the stress-life plot (S-N curve), typically beyond 10^6 fatigue cycles. For stresses below this fatigue limit, σ_e, there can be infinite cycles without failing. This value typically lies between 35% and 50% of the tensile strength for most steels. [31]

Many aluminium alloys, high strength steels and other materials do not have a plateau in their stress-life plot and show a continuously decreasing fatigue limit for a higher amount of cycles. This behaviour can be seen in the dotted line in figure 4.4.

Using Granta EduPack 2022 R2® the requirements are set out in multiple stages in order to obtain a shortlist of materials suitable for this design. Criterions for selection are EDM machinability, fatigue strength, density and tensile strength. This last stage is visible in figure 4.5
A material that satisfies these material requirements and which is often used in the industry for long-life flexure applications is Stavax®. This material is well machinable, a density of $7800kg/m^3$, has a Young's Modulus of 200GPa and a tensile strength of over 1500MPa [37].

4.2.7 Production method

As the design is relatively complex and the exact thickness of the thin, flexible parts is of high influence on the performance, a suitable production method is required. The choice is made for Travelling Wire Electrical Discharge Machining (EDM). This method can produce a high degree of shape complexity, because there is very little friction force delicate parts can be machined and minimum radii of 0.025mm can be achieved. It does require the material to be electrically conductive. [32]

4.2.8 Schematic

A schematic of the initial converter design is visible in figure 4.6. The hinges and other parts named here are referenced by these names in the remainder of this report.

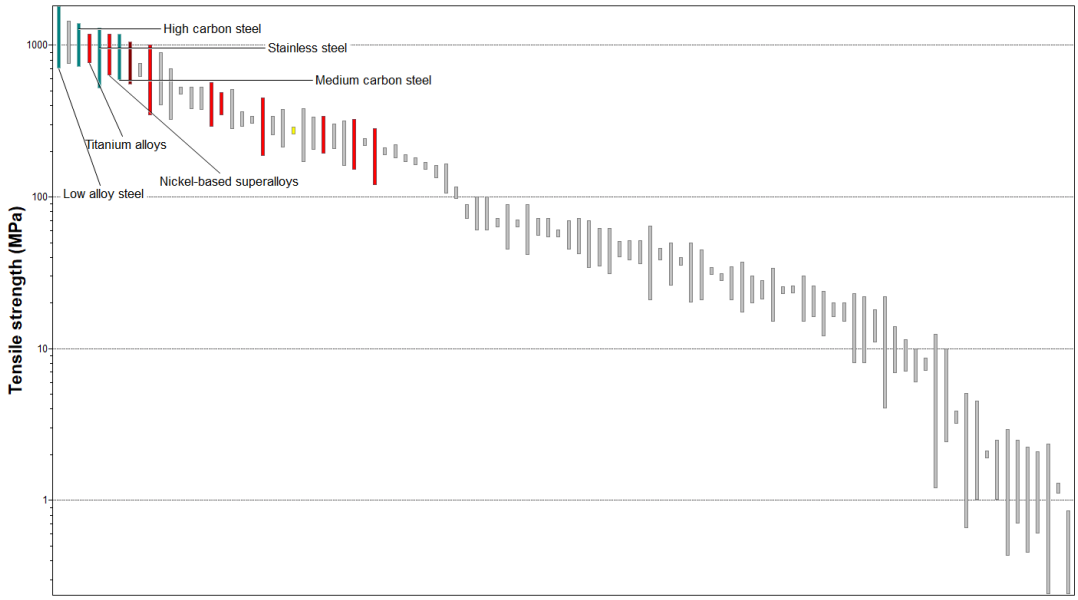

Figure 4.5: Last stage of the material selection in Granta EduPack 2022 R2. The best candidates are annotated. The grayed out materials have been disqualified in earlier stages of the selection.

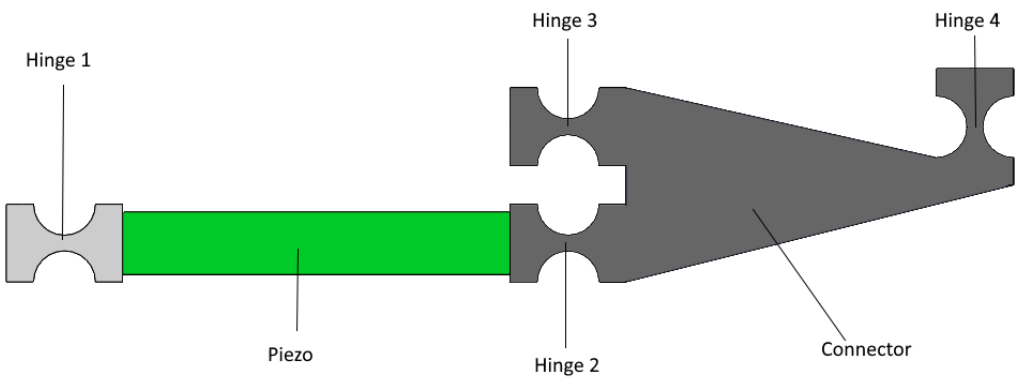

Figure 4.6: Initial design with parts named for future reference.

4.3 Sandwich plate

The sandwich plate is the part that is actuated by the converter and that creates the sound. It acts as the membrane in a loudspeaker. It consists of a honeycomb structured core and two face plates on either side.

4.3.1 Shape

In order to efficiently use the available space, a rectangular sound source is chosen. It is expected that the bending modes of the plate can be limiting for the frequency range in which the sound source is usable. The natural frequency of these bending modes is inversely related to the fourth power of the length of the sides, which is shown in the next chapter in equation 5.11 Therefore it is best to keep these as short as possible while retaining enough surface area to produce the required sound pressure levels. A square would be the obvious shape as it minimises the lengths of all sides. This, however, results in coinciding natural frequencies for the bending modes of the plate in both directions, which would increase its negative effects. Therefore the rectangular shape of previous designs like [33] is retained.

4.3.2 Sandwich structure

In previous work an elegant design solution has been found for creating a moving membrane which is both stiff and lightweight while also increasing the energy efficiency of the system. This is achieved by using a sandwich structured plate consisting of two face plates and a honeycomb core in between. The lower face plate is perforated, allowing air to move in and out, effectively increasing the volume of the enclosure by the volume air enclosed by the plate [33]. This sandwich structure is taken as the basis for the new design.

4.3.3 Equivalent plate

Modelling this sandwich plate in COMSOL increases the computation time significantly. Therefore it was chosen to convert the sandwich plate to a solid plate with equivalent properties. This is shown in figure 4.7.

In order to model the sandwich plate as a solid plate, a ”material” needs to be defined in COMSOL. The required properties for this are the Young’s modulus, the Poisson’s ratio and the density of the plate. Furthermore an equivalent thickness is to be determined.

According to [18], the equivalent density of a sandwich structure with to equal faces can be calculated by summing the masses of the parts and subsequently dividing by the equivalent volume:

$$m_{plate} = 2m_f + m_c \tag{4.1}$$

in which m_f is the mass of a single face plate and m_c is the mass of the core material. The mass of the faces is calculated by:

$$m_f = At_f\rho_f \tag{4.2}$$

in which A is the surface area of the face plate, t_f is the thickness of the face plate and ρ_f is the density of the face plate material. In this design two distinct face plates are used. For the top face plate, f_t, equation 4.2 can be used, whereas for the bottom plate a little adaptation is required, shown in equation 4.3:

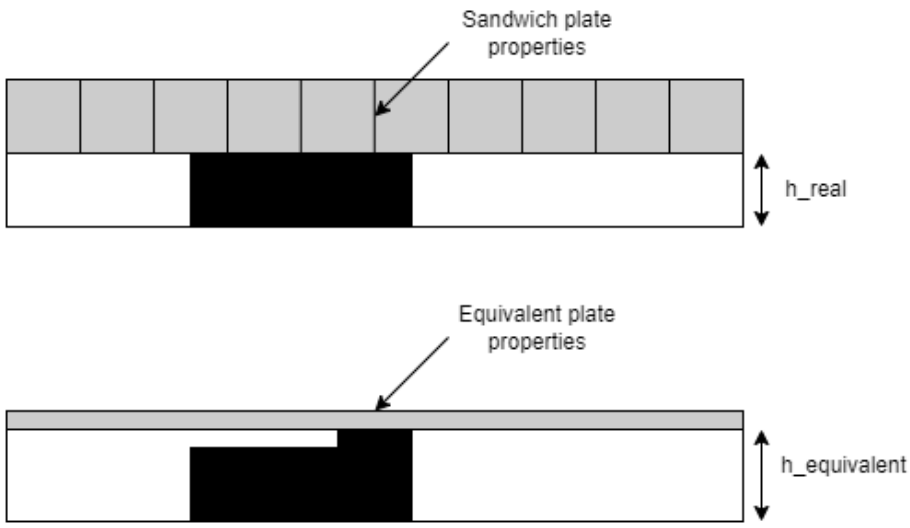

Figure 4.7: Modelling of the sandwich plate as a solid plate with equivalent properties in order to save computation time. The black box symbolises the converter to which a spacer is added in the lower case to keep it connected to the plate.

$$m_{f_b} = At_f \rho_{f_b}(1-q) \tag{4.3}$$

in which q is the perforation factor, which stands for the ratio of hole area to the total area of the plate.

The mass of the core part is determined by its geometry and the density of the material. Following figure 4.8, the density of the core can be expressed the density of the core material multiplied by a geometric ratio as follows:

$$\rho_{ca} = \frac{8dt_c}{A}\rho_c \tag{4.4}$$

In which d and t_c are shown in figure 4.8, ρ_{ca} is the average density of the core, ρ_c is the density of the core material and A is WL. [18]. Subsequently the mass of the core is the average density multiplied by its volume.

$$\rho_{eq} = \frac{m_{f_t} + m_{f_b} + m_c}{At_{eq}} \tag{4.5}$$

in which t_{eq} is the thickness of the equivalent plate and ρ_{eq} is the density of the equivalent plate.

For equivalent properties for the thickness and Young's modulus, the following equations need to be satisfied:

$$2t_f E_f = t_{eq} E_{eq} \tag{4.6}$$

$$\frac{1}{12}\left[(t_c + 2t_f)^3 - t_c^3\right] E_f = \frac{1}{12} t_{eq}^3 E_{eq} \tag{4.7}$$

For equations 4.6 and 4.7 the core part is assumed to have no contribution to the stiffness of the plate. In reality it will have a very small contribution but this is negligible [18].
Solving these equations for t_{eq} and E_{eq} gives the following expressions:

$$t_{eq} = \sqrt{3t_c^2 + 6t_c t_f + 4t_f^2} \tag{4.8}$$

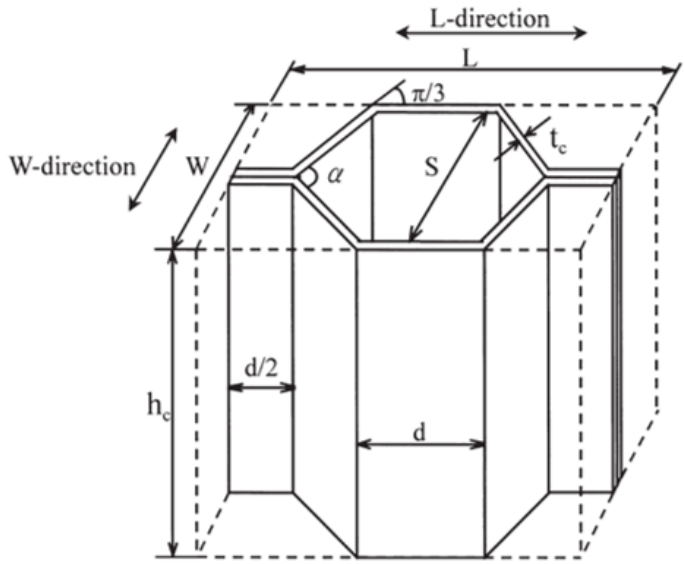

Figure 4.8: The geometry of a honeycomb unit-cell of the sandwich plate core with the relevant variables shown [18]

$$E_{eq} = \frac{2t_f}{t_{eq}} E_f \tag{4.9}$$

As this method assumes two equal faces, t_f in the formula for t_{eq} is assumed to be $\frac{t_{f_b}+t_{f_t}}{2}$ and in the formula for E_{eq} $2t_f$ is assumed to be $t_{f_b} + t_{f_t}$.
For the Poisson's ratio of the equivalent plate no clear expression could be found in literature. In order to circumvent extensive study into this expression its influence was analysed in the COMSOL model, which showed that the influence of its exact value is very small so long as no exotic properties such as negative ratios are chosen. Therefore a Poisson's ratio of 0.3 is assumed.

4.4 Box

The box is responsible for enclosing the air cavity in the acoustic source, for the suspension of the sandwich plate and which acts as a frame to which the converter is connected. The box consists of five walls and four rubber strips connecting the walls air tight to the sandwich plate.

4.4.1 Walls

The walls of the box have to be stiff and heavy in order to prevent vibrations from the inside to get out. The material should also add some damping to the system. A material commonly used in loudspeakers is MDF. MDF is both stiff and heavy and has a relatively high sound absorption coefficient (0.1-0.2 depending on frequency range) [12].

4.4.2 Rubber strips

The rubber strips connect the plate to the walls of the box. These should separate the inside of the box from the outside, sealing the air cavity inside. The strips also exert forces on the plate when it is displaced, giving it some guiding. The exact properties of the strips are deemed not critical and therefore the rubber strips are copied from [33]. A slight inaccuracy in this paper was

discovered and this was adjust before copying. As the Young's Modulus of the rubber in both lengths of strip is the same, the longer edge has a higher resistance (92.3Nm^{-1}) to displacement of the plate than the shorter edge (65.3Nm^{-1}).

5 DESIGN ITERATIONS

In this chapter the design decisions of the previous are turned into simulation designs in COMSOL. Simulations are run on (parts of) the simulation designs and conclusions are drawn form the (sub)results. These conclusions are subsequently used to create new designs on which simulations are performed again. This is iterated until a design is found which satisfies the requirements. The dimensions in the figures change more than which is discussed. These figures were made during the process of designing and iterating. This process happened by continuously improving different parts, going back to parts previously improved to see if there is even more room for improvement etcetera. As presenting the process in this way would result in a chaotic report, it is not presented in chronological order, but rather divided per subpart. Therefore the designs and dimensions vary more than just what is discussed in each section.

Ideally all parameters would be varied against all other possible configurations of parameters in simulations to produce an optimal configuration. As there are many design parameters, this would take a huge number of simulations and is therefore not possible. By making assumptions about relations between parameters being continuous for instance, it is possible to use optimisation algorithms that require much less simulations, though still too many, and these assumptions would have to be verified. The choice was therefore made to not vary every parameter for every configuration. Instead many were varied individually in a fixed configuration. This fixed configuration would be changed according to the conclusions of the performed optimisation before optimising the next parameter. For most parameters this method would find a rough optimum, though some parameters were connected in a more complex way. Increasing some parameter A to its found optimum would decrease the optimum of parameter B, while decreasing parameter B would decrease the optimum for parameter A. In this case the parameters were varied together in a further fixed configuration. This was specifically the case with the widths of the hinges.

5.1 Initial simulation design

For the initial design, three things were considered. For the dimensions of the piezo, the optimum found in [34] was used. For the hinges, notch hinges were chosen. Initially all hinges were designed to be exactly the same and the dimensions were estimated from [34]. For the dimension of the connector, an amplification factor was estimated which was required to achieve the required motion of the plate given the motion of the piezo. Besides these considerations, no optimising was conducted yet.

As the problem with the previous design was thought to be in the conversion mechanism, the initial design only consists of this mechanism. This design can be seen in figure 5.1.

5.1.1 Results and conclusions

The first natural frequency of the converter was found to be 1182 Hz and the highest stress that occurs is 6 MPa. The vertical displacement of the plate is simulated to be 120 μm. These results would suffice the requirements and therefore the initial design seems very promising.

Figure 5.1: Initial design. The notch hinge on top is connected to the moving plate, the other two notch hinges are connected to the ”fixed world”

Figure 5.2: Initial design with added frame connecting it to the ”fixed world” to include its influence

From this it can be concluded that the conversion mechanism has no problematic internal natural modes. Improvements are definitely possible, but first the model has to be expanded in order to find other possible problems.

5.2 Improvements

Based upon the promising results of the initial design, the model is first expanded to also include the frame which connects the converter to the ”fixed world”. Afterwards improvements on the connector, hinges and piezo are considered. Next, the sandwich plate and the enclosure of the air cavity are added. In this section these additions, their consequences and some optimisations in their regard are discussed.

5.2.1 Frame

As the ”fixed world” in the initial model does not really exist and a frame is required to connect the converter to the base of the acoustic source, this is added. In order to make fabrication easier and to reduce misalignment, both the frame and the converter are made as one part by travelling wire EDM. Therefore the material of both has to be the same.

A first design of the mechanism with frame can be seen in figure 5.2. Running static simulations in this configuration showed that the vertical motion of the top of the converter was reduced significantly after adding the frame. Inspection of the results showed that the frame would bend downward and that that caused the vertical motion to be reduced, as can be seen in figure 5.3.

Increasing the thickness of the frame would reduce this the bending a little, but not enough. Making the frame out of a stiffer material was also considered, but this also did not achieve the desired result. When trying these options it was also found that sideways bending of the frame would be problematic, as can be seen in figure 5.4.

Figure 5.3: Side view of the bending of the frame and converter which results in decreased vertical motion of the plate.

Figure 5.4: Top view of the sideways bending which causes an additional natural mode.

As changing the dimension and shape of the frame itself did not result in sufficient improvement, another solution had to be found. Adding supports on either side of the frame was considered as in figure 5.5. This negated the reduction in vertical motion and simultaneously prevented the sideways bending.

5.2.2 Connector

In the initial design the connector consisted of a rectangular block. The ideal connector would have infinite stiffness while having no weight. Also the connector has to cause a high amplification of piezo movement to vertical movement while not exceeding maximum piezo forces and not exceeding the allowable stresses in the hinges.

In order to reduce weight without reducing the stiffness, non load-bearing mass is cut away. The stresses in the connector are shown in figure 5.6. From this it is clear that the stresses concentrate around the hinges. In the model in the figure, the sandwich plate is not yet added, but a similar stress pattern around the hinge is expected. Taking this into account, the lower right corner does not seem to contribute and can therefore be cut off. This is shown in figure 5.7.

Reducing the total thickness of the converter further is possible by lowering hinge 4. By lowering the hinge point to the same height as the hinge point of hinge 3, parasitic horizontal motion of hinge 4 is also reduced. This version can be seen in figure 5.8.
In order to reduce the mass even further, it was considered to perform a topological optimisation on the connector. This would likely lead to a hole in the middle of the part. However, simulation show that artificially setting the weight of this part to 0 has very little impact on the relevant natural frequencies, therefore this optimisation is left for further research.

As the height of the connector is defined by the thickness of the actuator, the thickness of the frame and the room between them, the dimension to be optimised is the length. Because the connector acts an amplifier to the displacement of the actuator, its length is largely deciding for the stroke of the diaphragm. A larger connector results in a larger stroke. A larger connector however is also more compliant and results in lower natural frequencies. Relatively early in the design process the dimensions of the rectangular connector were optimised with a minimum stroke and as high as possible stroke. After ordering the parts and while waiting for them to

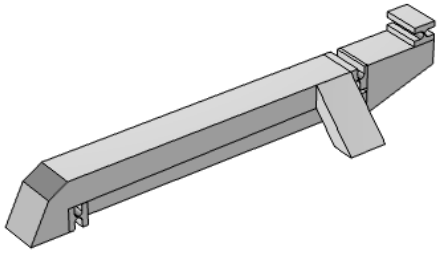

Figure 5.5: Supports are added on either side to prevent the undesired motions of the converter and frame

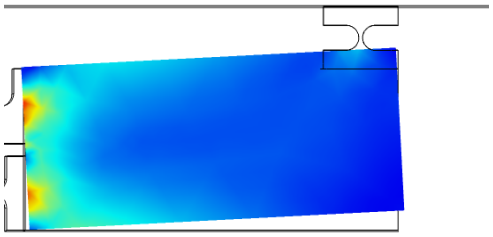

Figure 5.6: Von Mises stress in initial connector

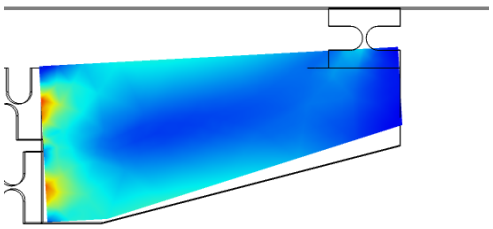

Figure 5.7: Von Mises stress in reduced-weight connector

arrive, the optimisation was performed again on the latest version of the design. The results of both optimisations are visible in figure 5.9. From this figure it is clear that the dimension corresponding to the optimal natural frequency changed significantly.

5.2.3 Prestress mechanism

Though the initial prestress mechanism was found to exert enough compressive force on the piezo to prevent undesired forces to affect it, there were some concerns. As the displacement required to reach the desired preload, a small misalignment would already have large consequences. As a result of this, it was decided to redesign the prestress mechanism to be more robust. In this redesign, the difference between the excited position and the initial position is relatively small compared to the strain induced during assembly. This means that a little misalignment will only cause a small difference in strain compared to the designed strain, making it more robust. This redesigned prestress mechanism is visible in figures 5.10 and 5.11.

The prestress mechanism is also subject to fatigue and therefore cannot exceed certain stress

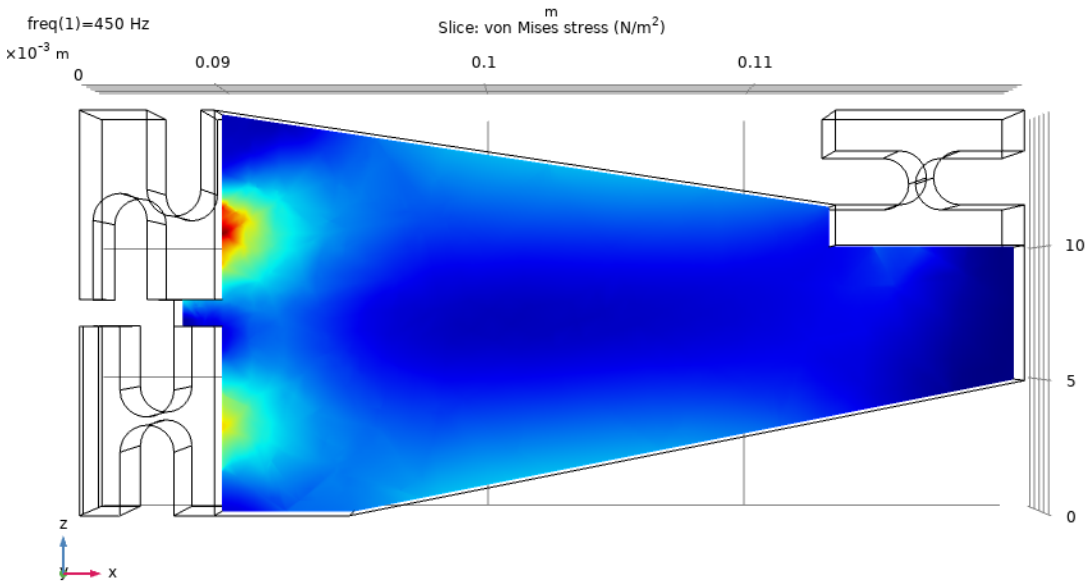

Figure 5.8: Von Mises stress in the lowered connector. The stress levels shown are far below the maximum allowable stress.

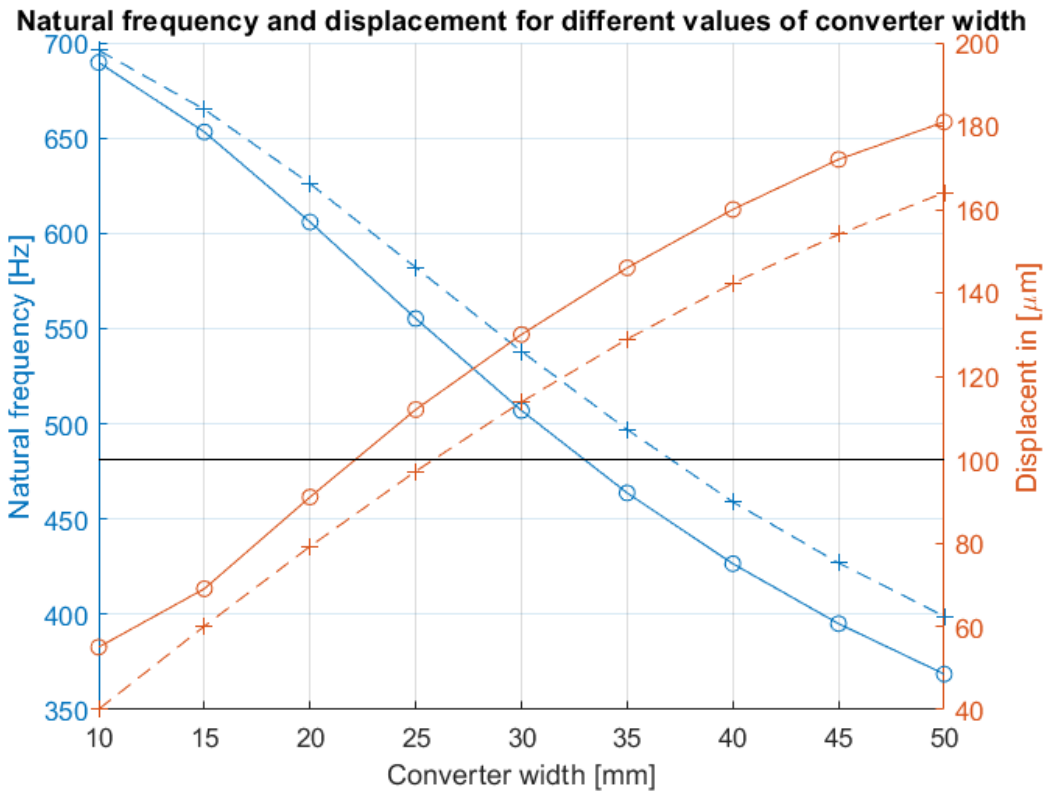

Figure 5.9: Natural frequency and displacement as functions of the converter width. The dashed +-lines are the early optimisation, the solid o-lines are the result of an optimisation on the final configuration. The solid black line is the minimum displacement given in the requirements.

levels for infinite fatigue life. The amount of stress in the prestress mechanism is mostly determined by the prescribed displacement. It was found that 0.8mm displacement is needed in the new model to provide the required 10MPa prestress on the piezo. In figure 5.12 it can be seen that this displacement is achievable without exceeding the the fatigue limit during operation.

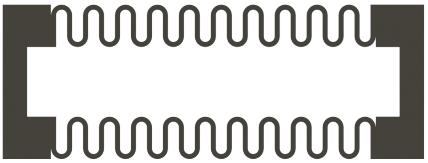

Figure 5.10: The final design of the prestress mechanism, designed to be more robust.

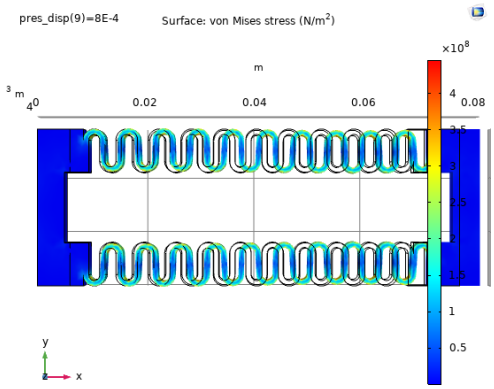

Figure 5.11: Stresses in the final prestress mechanism at maximum excitement.

5.2.4 Hinges

The notch hinges were all equal in dimensions in the initial design and the stresses in the hinges were much lower than the maximum allowable stress. Therefore the thickness of the hinges can be reduced, decreasing the stiffness and thereby the required actuator force, without exceeding the maximum allowable stress. Aside from the maximum allowable stress, fabrication through travelling wire EDM limits the minimum thickness of components. Because of this, the thickness of all the hinges was reduced to 0.25mm.

Simulations showed that the stresses in the hinges increased significantly, but only in the case of hinge 3 the maximum allowable stress was exceeded. In order to reduce the stress in this hinge, the hinge was placed under an angle. Varying the angle resulted in the stresses which can be seen in figure 5.13. From this it can be concluded that an angle of $34°$ is favourable.

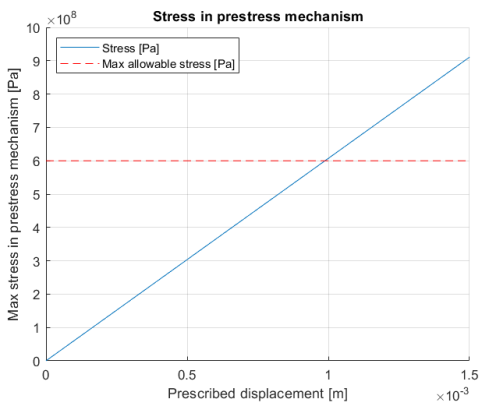

Figure 5.12: The maximum stress in the prestress mechanism as a function of the prescribed displacement.

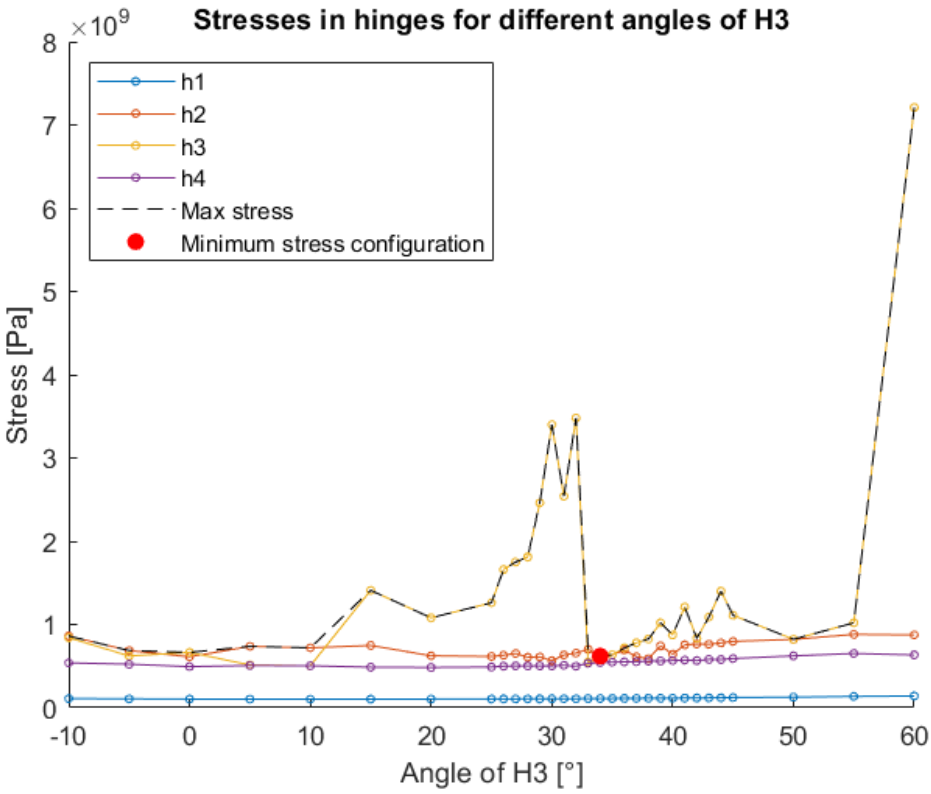

Figure 5.13: The maximum Von Mises stress at 450Hz in the hinges when hinge 3 is placed under various angles. An angle of around 34 degrees results in minimum stresses.

In order to explain the sharp increase in stress in hinge 3 around the angle of $30°$, the hinge is sectioned to see how stress concentrations behave at different angles. It was expected that the stress concentration might migrate through the hinge. A mesh refinement and further inspection of the section views in figure 5.14 did however not show this migration and did not provide a clear explanation.

As this inexplicable sharp increase in stress puts doubt on the validity of the model, the same optimisation was performed once more on the final design and with a much finer mesh grid. This optimisation yielded the results visible in figure 5.15. The corresponding relevant natural frequencies can be seen in figure 5.16.

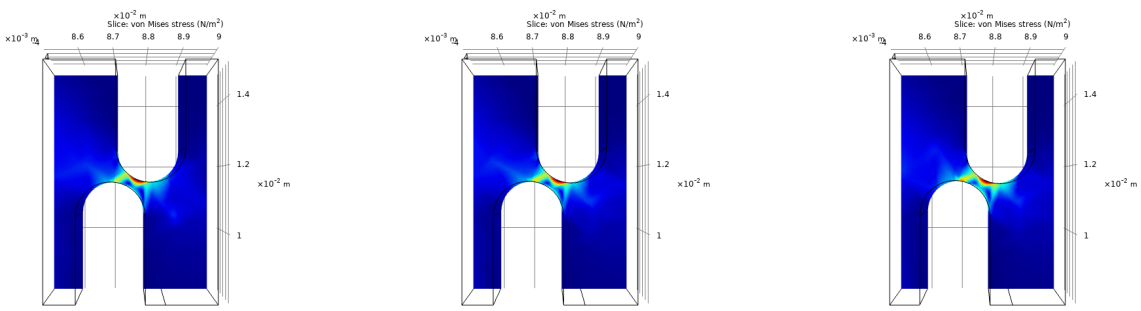

Figure 5.14: Section views of the stress in hinge 3 in excited position. The angle θ of hinge 3 is from left to right respectively $30°$, $32°$ and $34°$

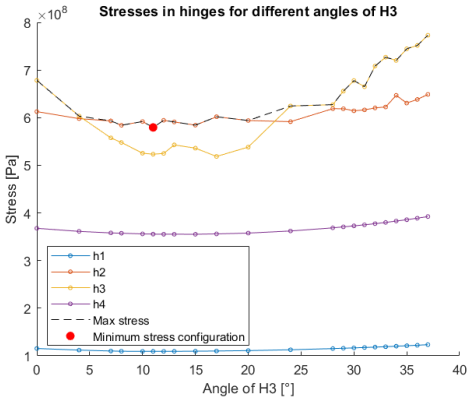

Figure 5.15: Optimisation of the angle of Hinge 3 performed on the final design, which yields much smoother results and a very different optimal angle.

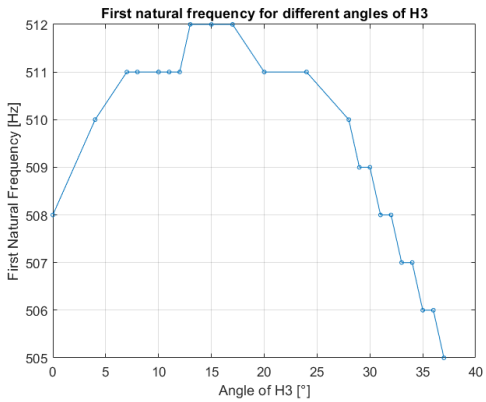

Figure 5.16: The first natural frequency of the system for various angles of Hinge 3. Its influence is only minor, but the optimal angles in this respect correspond to the optimal angles for the stresses.

The changes in hinge thickness and the angle of hinge 3 caused the stress division throughout all the hinges to change, in some cases increasing to over the maximum allowable stress. In order to keep stresses below the fatigue strength, an optimisation was performed on all hinges. For each hinge two factors were taken into account: the thickness of the wall in the middle and the radius of the notch.

Simulations of varying notch radii show two distinct effects. Firstly, a smaller radius corresponds to a higher first natural frequency, as visible in figure 5.17. This is as expected as a smaller notch makes the hinge stiffer. Secondly, the stresses in the hinges change with varying radii. This relation is more complicated, as can be seen in figure 5.18. From the first relation it is clear that a smaller radius is better for performance, while the second relation shows a minimum around 2.2mm radius. From this it is concluded that a radius of 2.0mm is best for this design.

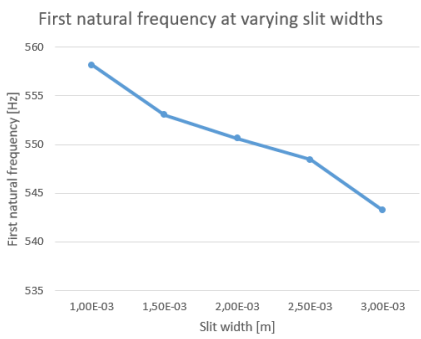

Figure 5.17: The first natural frequency of the system for varying notch radii c.q. slit widths. A smaller radius corresponds to a higher natural frequency.

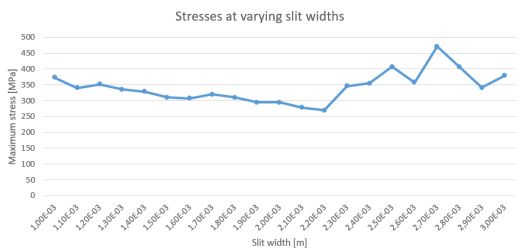

Figure 5.18: The maximum stress in the system for varying notch radii c.q. slit widths. The lowest stress occurs around 2.2mm radius.

In order to assess whether the found stresses in the model can be deemed plausible, a simple calculation is performed based on equations in [28]:

$$\beta = \frac{t}{2a_x} \tag{5.1}$$

In which β is a geometric factor for notch hinges, t is the thickness of the hinge and $2a_x$ is the length of the hinge. As hinge 3 is the hinge with the highest stresses a hand calculation is performed for this hinge.

$$\sigma = K_t \frac{6M}{t^2 b} \tag{5.2}$$

In which b is the depth of the spring, M is the moment applied to it and according to [28], if $\beta \leq 0.23$, the following equation holds for K_t:

$$K_t = (1+\beta)^{\frac{9}{20}} \tag{5.3}$$

The moment applied is the force that the actuator delivers when extending multiplied by the lever. This is in the order of $1000N$ multiplied by $8e-3$m. The thickness is $3e-3$m and the depth is $10e-3$m. This results in a stress of 565MPa, which is in the same order of magnitude as the simulated results, which therefore seem plausible.

5.2.5 Piezo

In the initial design, the first natural frequencies were bending modes of the piezo. These frequencies were above the required range, but only slightly. Changes in the design could reduce this and thereby limit the usable frequency range of the acoustic source.

Reducing the length of the piezo increases its stiffness. However it also decreases its motion range, which reduces the vertical motion of the plate and thereby the maximum sound pressure levels that can be achieved. Different lengths of piezo are simulated and based on the resulting motion and stiffness the optimum length is chosen.

5.2.6 Sandwich plate

The sandwich plate is added to the model with the same properties as the sandwich plate in [33]. In order to add the plate to the system, the connection to the ”fixed world” also has to be modelled. This connection consists of rubber strips. These strips are modelled as a stiffness matrix added to the sides of the plate. The properties of these strips are also taken from [35].

5.2.7 Stiffness of air in cavity

To model the plate and its behaviour properly, the influence of the enclosed air cavity has to be modelled as well. Under the first natural frequency, the moving plate acts as a piston. Because of this, the air in the enclosure can be modelled as a spring which is excited by the motion of the plate.

The change in pressure from an equilibrium pressure is related to the volume change of a fluid by the compressibility, κ [17]:

$$P - P_0 = p = -\frac{1}{\kappa}\frac{dV}{V_0} \tag{5.4}$$

multiplying both sides by the surface area of the plate, the net downward force on the plate can be found.

$$pA = -\frac{A}{\kappa}\frac{dV}{V_0} = F \tag{5.5}$$

in which:

$$dV = V_t - V_0 = lwh(t) - V_0 \tag{5.6}$$

in which lw is the surface area of the plate, $h(t)$ is the height of the plate as a function of time and V_0 is the reference volume, which is equal to lwh_0. Also $h(t) - h_0 = \Delta h$. Substituting these relations gives:

$$-\frac{lw}{\kappa}\frac{\Delta h}{h_0} = F \tag{5.7}$$

Stiffness k can then be found by using Hooke's law::

$$F = -kx \tag{5.8}$$

in which x is the displacement distance, which in this derivation is Δh. Substituting in equation 5.7 and rewriting gives:

$$k_{air} = \frac{lw}{\kappa h_0} \tag{5.9}$$

When evaluating this expression it has to be noted that h_0 is the height of the air cavity, which as explained in the previous chapter includes the volume of the air in the sandwich plate. For the model k_{air} equals roughly 2.16×10^5 N/m.

Consequences

The addition of the sandwich plate, rubber suspension and air cavity to the mechanism have a negative effect on the system's behaviour. An Eigenfrequency study in COMSOL shows many low frequent modes related to the plate, which can be seen in figure 8.3. The modes 5.19a, 5.19b, 5.19c and 5.19e are rigid body modes of the plate. These should not be problematic as long as the system is excited symmetrically. This can clearly be seen in figure 5.20.

5.3 Sandwich plate improvement

The first natural frequency that is coupled to the first non-rigid body mode is limiting for the frequency range in which the acoustic source can be used. Through simulations in COMSOL, it seemed that this first mode was connected to the first bending mode of the sandwich plate. This mode shape can be seen in figure 5.19d. In order to solve this, different approaches have been attempted:

5.3.1 Different equivalent plate

In the conversion of the sandwich plate to the equivalent solid plate of the previous chapter, some assumptions were made in order to use equations for two equal faces for this case with two different faces. As this might have caused inaccuracies, another approach was sought.

The thickness of the equivalent plate is chosen to be equal to the thickness of the sandwich plate and only the face plates are assumed to have a contribution to the stiffness. This changes equation 4.9 to the following:

$$E_{eq} = \frac{t_{f_b}E_{f_b} + t_{f_t}E_{f_t}}{t_{eq}} \tag{5.10}$$

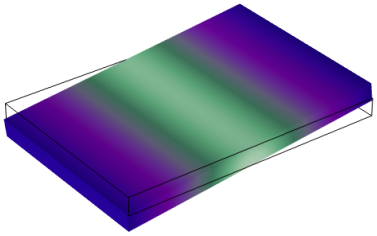

(a) 252Hz

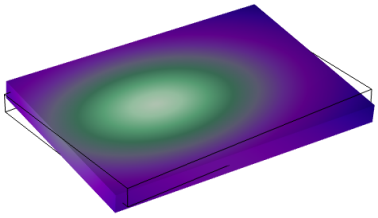

(b) 259Hz

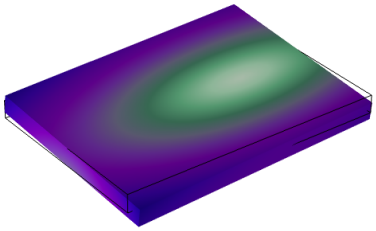

(c) 263Hz

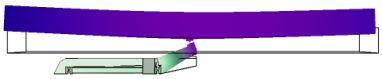

(d) 375Hz

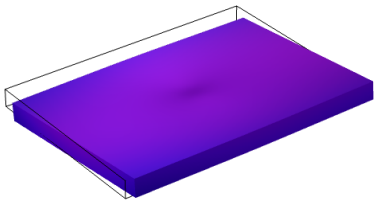

(e) 704Hz

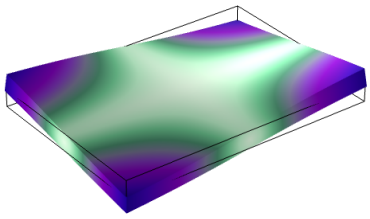

(f) 814Hz

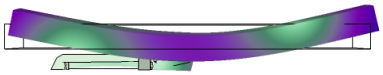

(g) 909Hz

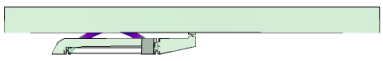

(h) 1031Hz

Figure 5.19: The first 8 natural modes of the system with their respective natural frequencies.

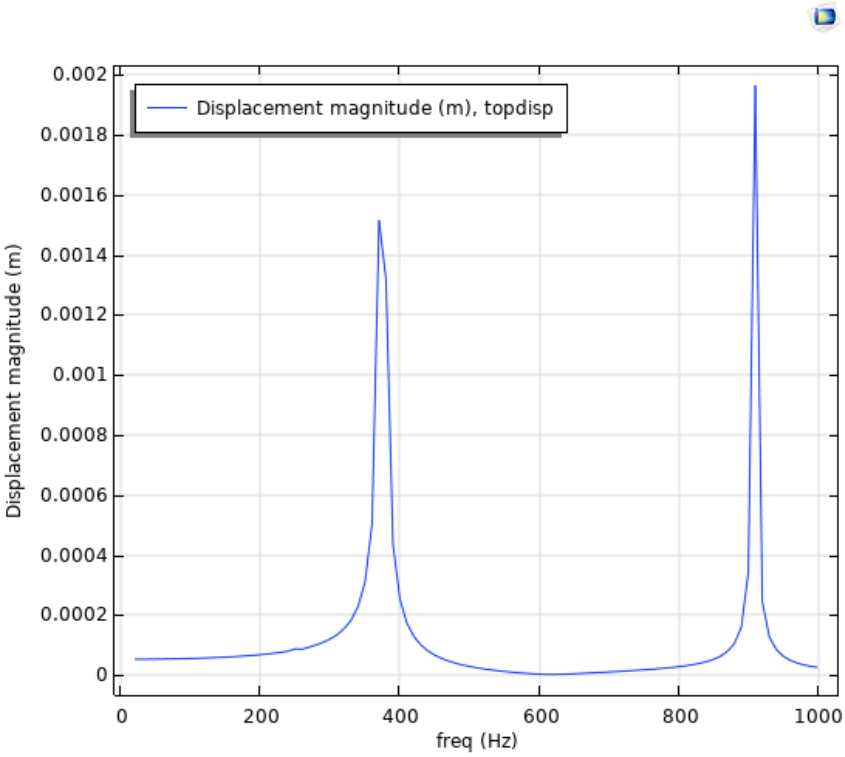

Figure 5.20: Frequency response of the mechanism, with clear peaks around the frequencies responding to the modes in 5.19d and in and 5.19g

5.3.2 Local stiffening

In order to increase the stiffness against bending, local stiffening could be added. Small beams could be added in the at positions where the most bending occurs in order to make it stiffer. Alternatively, a small extra plate could be added in the highest bending regions in the middle of the sandwich plate. Both methods which should increase the stiffness of the plate can be seen in figures 5.21 and 5.22.

Whereas these method should increase the stiffness, more than the increase in mass, simulations show that the natural frequency decreases due to these additions.

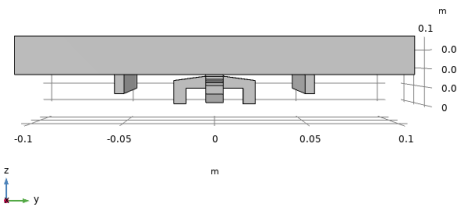

Figure 5.21: Beams are added to the plate to increase the stiffness

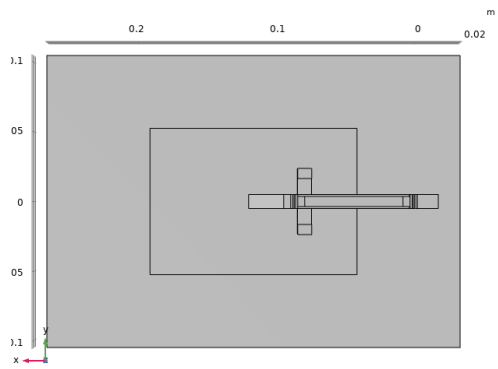

Figure 5.22: An extra plate is added to the plate to increase the stiffness

5.3.3 Increasing plate thickness

Another option is to increase the thickness of the sandwich plate itself. This would increase the stiffness by the third order while only increasing the weight by the thirst order. This however would also increase the total thickness of the construction, which is not desirable. Performance does outweigh small thickness in importance, so if needed, this could be used.

Simulations in this case again show results which are contrary to the expectations. Increasing the thickness of the plate again decreases the natural frequency.

5.3.4 Core fraction optimisation

As the plate is taken from previous work like [33], no optimisation has been conducted yet. In order to retain the effect of the air within the plate as part of the total enclosed volume of air, the only variable is the fraction of core material. When modelling the plate as a simply supported wide beam, the natural frequencies, corresponding to the beam bending modes can be found by the following equation [3]:

$$f_n = \frac{K_n}{2\pi}\sqrt{\frac{EIg}{wl^4}} \tag{5.11}$$

in which f_n is the natural frequency corresponding to the nth mode, I is the moment of inertia, l is the length of the beam g is the gravitational acceleration, E is the Young's modulus, w is the uniformly distributed load including the beams weight and K_n is a constant corresponding to the nth mode. For this optimisation the only mode of interest is the first. The corresponding value K_1 is 9.87 [3].
When only taking the mass of the plate into account and neglecting the distributed stiffness from the air in the cavity, the load w can be expressed as:

$$q = \rho_l g \tag{5.12}$$

in which ρ_l is the density per unit length of the beam, which can be calculated through:

$$\rho_l = \frac{m_{plate}}{l} = \frac{m_c + m_f}{l} \tag{5.13}$$

While expressions for m_c and m_f were already derived before, an expression as a function of the core fraction i is required for this optimisation.

$$m_c = ilwh_{plate}\rho_{ca} \tag{5.14}$$

in which ρ_{ca} is the same as in equation 4.4, and l, w and h_plate are the length, width and height of the plate respectively.

$$m_f = (1-i)ldh_{plate}\rho_f \tag{5.15}$$

For this optimisation two equal faces are again assumed. Results will differ slightly for the different faces, but the relation between core fraction and behaviour remains the same.
Now expressions for E and I are required as a function of the core fraction:

$$E_{plate} \approx (1-i)E_f \tag{5.16}$$

$$I_{plate} \approx \frac{1}{12}w_{plate}[h_{plate}^3 - (ih_{plate})^3] \tag{5.17}$$

Using these relations gives the blue line in figure 5.23.

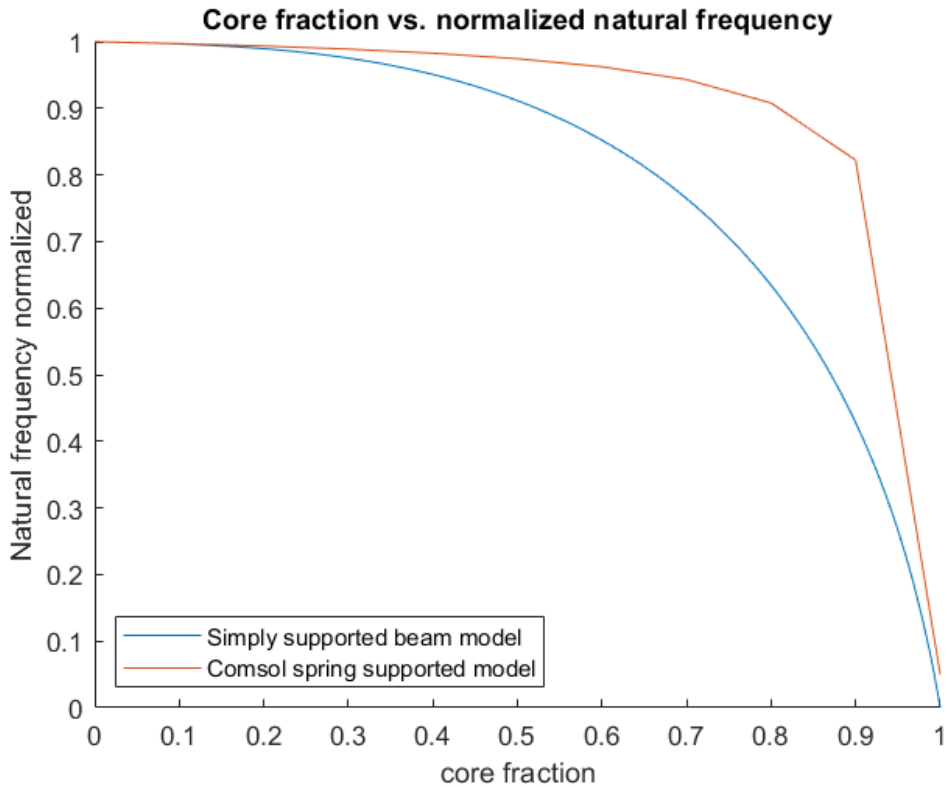

Figure 5.23: Normalised first natural frequency as a function of the fraction of core material modelled by equation 5.11 and modelled in COMSOL

As the real mechanism is not only subject to its own weight, but also to the distributed spring load of the air, a simple COMSOL model is made with this distributed stiffness. The result of this is the red line in figure 5.23. The behaviour of the real case lies somewhere in between these two lines.

From this figure three main conclusions can be drawn. First: the more solid the beam becomes, the higher the natural frequency becomes. Second: The decrease in natural frequency is relatively small until around $i = 0.7$, therefore weight of the plate can significantly be reduced from the weight of a solid plate without losing too much performance. And thirdly and foremost: the ratio of core material of around 0.98 in previous work like [33] is far from optimal for stiffness against bending.

In order to assess the effectiveness of decreasing the core fraction in the sandwich plate, simulations were performed. Like the other options however this again gave counter intuitive results, as the natural frequency decreased with increasing core fraction, as visible in 5.24. Further investigation of the mode in figure 5.19d is therefore required.

5.3.5 Weight reduction

Further investigation, showed that not the stiffness of the plate is the most influential on the mode in figure 5.19d, but the weight of the plate. This leads to the conclusion that this mode is in fact not the first bending mode of the plate. Increasing the stiffness of the piezo and the connector in simulations results in increased natural frequencies. Decreasing the weight of the plate has similar effects.

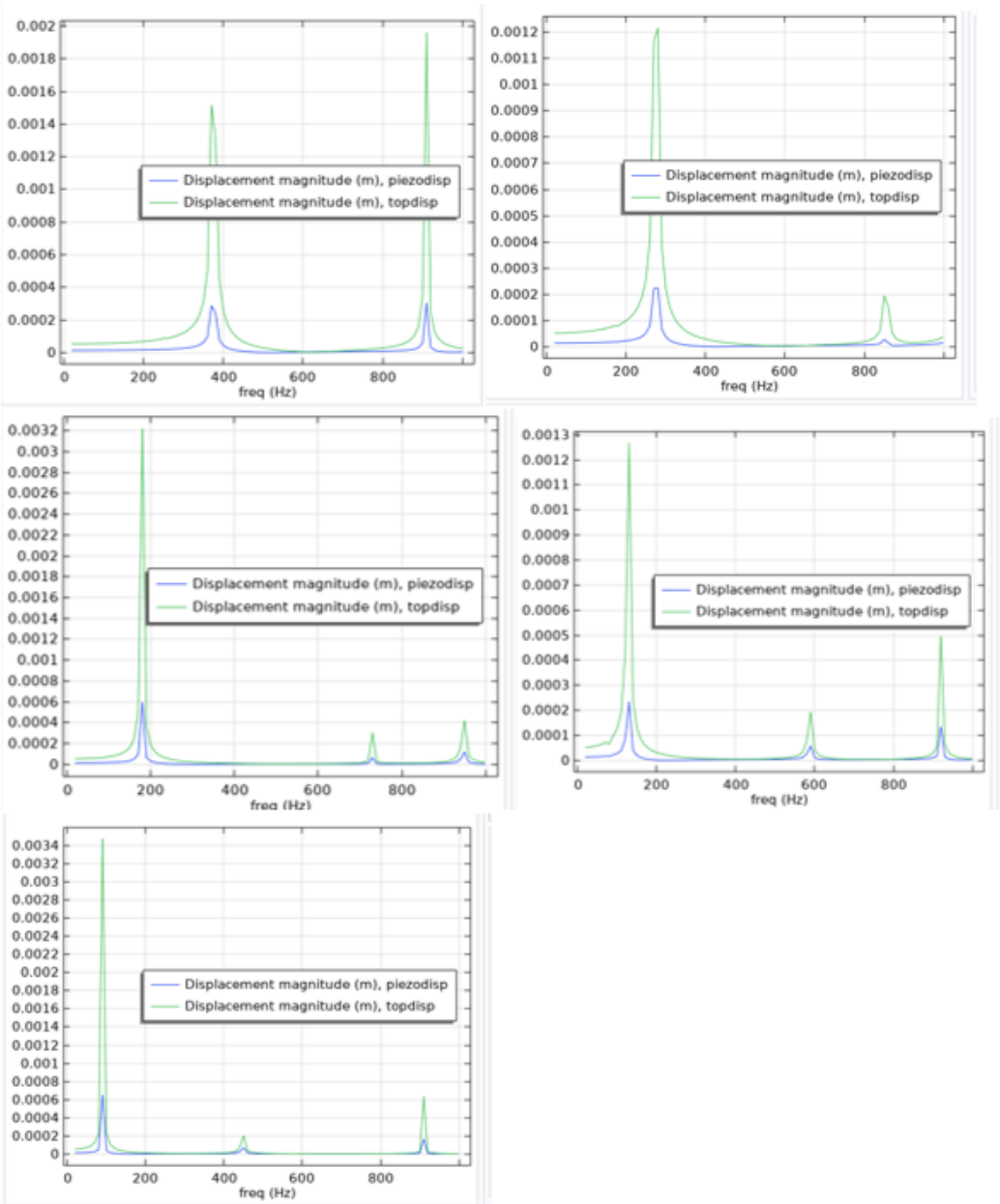

Figure 5.24: Frequency response of the system different core fractions. Upper left $i = 0.99$, upper right $i = 0.98$, middle left $i = 0.95$, middle right $i = 0.90$, lower left $i = 0.80$. The first natural frequency is clearly decreasing with a decreasing core fraction.

While increasing the stiffness of the converter in simulation is easy, in practice this would require very exotic material properties or an increased thickness of various parts which would in turn increase the weight, negatively affecting the natural frequencies.

On the other hand, a weight reduction in the plate might be achieved more easily. The thicknesses of the face plates are already very thin (0.125 and 0.2mm respectively), making these thinner would introduce manufacturing difficulties. The core material could be improved upon significantly though.

The core material used in previous works like [33] is an aluminium honeycomb structure with 13mm wide hexagons and 0.1mm thick walls. This core material has a density of 77kg/m^3. For readily available honeycomb plate material this an average density, though special lightweight construction materials do exist with even lower densities. An example of very lightweight honeycomb material is EasyComposites® Aluminium Honeycomb with cells of 19.1mm width. This has a density of 28.8 kg/m^3. This material has a wide range of applications and is advertised to be available [9]. An even lower density core material is NOMEX® honeycomb - commercial 6.4mm cell size. This material has a density of 24 kg/m^3. This material consists of aramid fibre paper impregnated with a heat resistant phenolic resin. This material is more exotic than the aluminium core and is suggested for use in aeronautics and in military applications amongst others [29].

5.4 Final design

The conclusions drawn in this chapter for the individual parts are put together in a final design, the performance of which is to be assessed both in simulation and in physical testing. The final design of the motion conversion mechanism consisting of piezo, prestress mechanism, converter and supports is shown in figure 5.25. The relevant dimensions can be found in the technical drawing in the Appendix. This drawing is for the model that is actually manufactured and because of the reasons explained in chapter 7 differs slightly form the optimal model. The dimensions that differ are the converter width (25mm as opposed to 30mm in the drawing), the angle of hinge 3 (11$\circ$ as opposed to 34$\circ$) and the thicknesses of hinge 2 (0.2625mm as opposed to 0.3mm). The frequency response can be seen in figure 5.26. The first non-rigid-body natural frequency is found at 557 Hz, as visible in figure 5.27 and in order to remain under the maximum allowable stress, 600MPa, the operational bandwidth is 20-500 Hz.

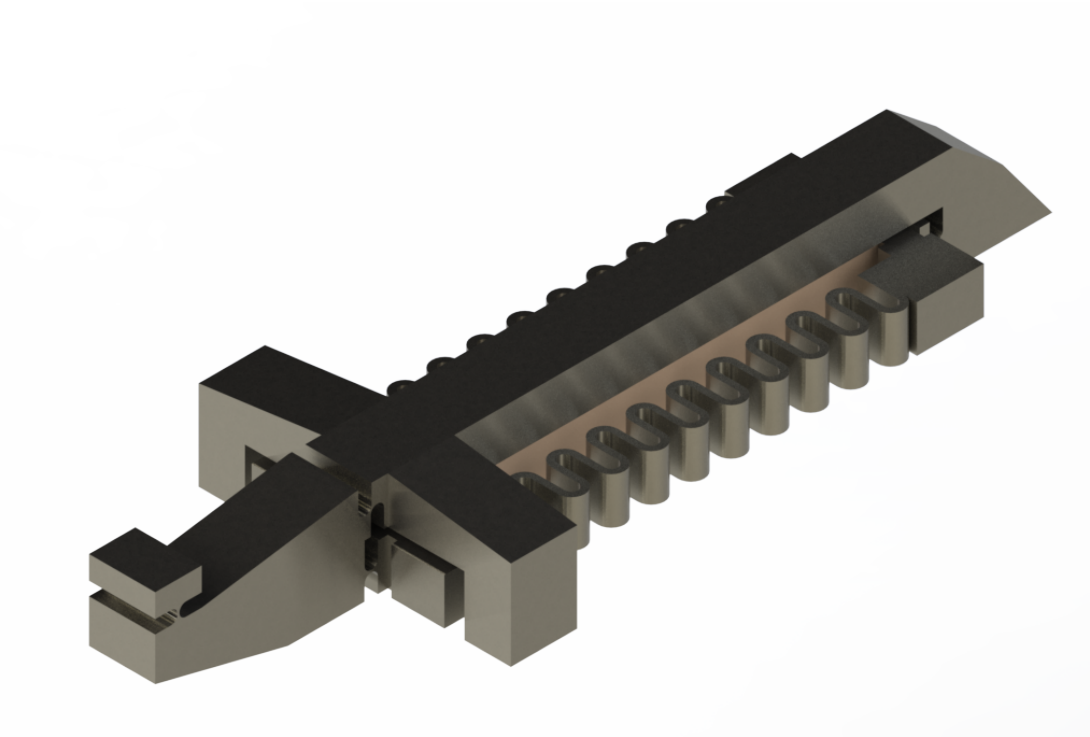

Figure 5.25: The final design of the motion converting mechanism based on the conclusions of this chapter

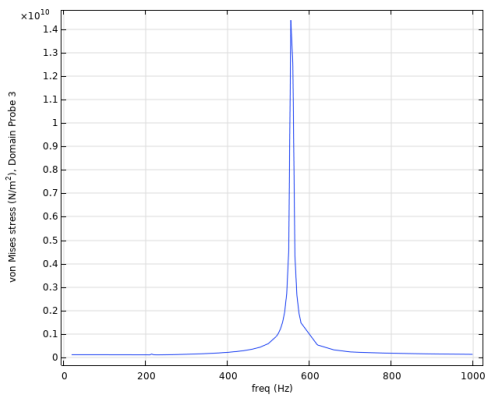

Figure 5.26: Frequency response of the final model. Up to 500 Hz the stresses remain under 600 MPa, which is the fatigue limit.

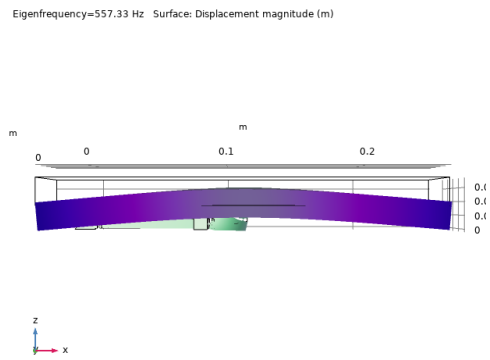

Figure 5.27: The first mode affecting the frequency response is the mode corresponding to the first not-rigid-body-mode at 557Hz.

6 ACOUSTICS

In this chapter the acoustic aspects of the design are discussed. During the design, the actual sound generation has for the most part been left out. The most important occurrence is in the natural frequencies of the system, interfere with the desired sound generation. However these are also of great influence on the stresses in the system and have therefore already been taken into account previously.

Another important aspect of the actual sound generation are the sound pressure levels (SPL) generated. This has not yet been taken into account explicitly, although it is implicitly represented in the design requirements. There it was stated that the minimum displacement of the plate has to be 100μm. In this chapter the reasons behind this requirement and its effect are discussed.

6.1 Acoustic modelling

Aside from predicting natural frequencies and determining stresses, the COMSOL model can also be used to predict the SPL's that are generated at different frequencies. In order to verify that these predictions make sense, the Rayleigh integral is implemented in a Matlab model. The general form is [14]:

$$\hat{p}(x,y) = \frac{j\omega\rho}{2\pi}\int_S \frac{v(S)e^{-jkr}}{r}dS \tag{6.1}$$

In which S is the surface of the moving piston, v(S) is the normal velocity and r is the distance to the observer. For low frequencies the acoustic behaviour can be approximated by a circular piston with an infinite baffle. In order to do so, the following equation is implemented [26]:

$$p_\omega(r) = -ik\rho c\frac{e^{ikr}}{4\pi r}f_\omega(\theta), \quad f_\omega(\theta) = 2u_\omega\pi a^2\left[\frac{2J_1(ka\sin(\theta))}{ka\sin(\theta)}\frac{\cos(\theta)}{\beta+\cos(\theta}\right] \tag{6.2}$$

$$k = \frac{\omega}{c} = f\frac{2\pi}{c} \tag{6.3}$$

In which $u_\omega e^{-i\omega t}$ is the normal velocity inside a circular piston of radius a corresponding to the same surface area as the rectangular speaker, centred around the origin and zero over the rest of the plane $z = 0$, r is the distance from the centre of the piston to the observation point, θ is the angle from the normal to the plane at the centre of the piston to the observation point. And in which k is the wave number, c is the speed of sound, ρ is the density of the medium, f is the frequency and J_1 is the Bessel function of the first kind. Boundary plane $z = 0$ can react to pressure waves by moving if it is not completely rigid. This happens with point impedance $z(\omega) = \rho c/\beta$. In case the wall around the piston is near rigid, the impedance is high, meaning β is very small and a the term in equation 6.2 involving β becomes nearly unity [26]. For $\theta = 0$, the term in brackets in equation 6.2 becomes unity. This means that for a rigid wall the pressure directly in front of the source at distance r can be obtained through the following:

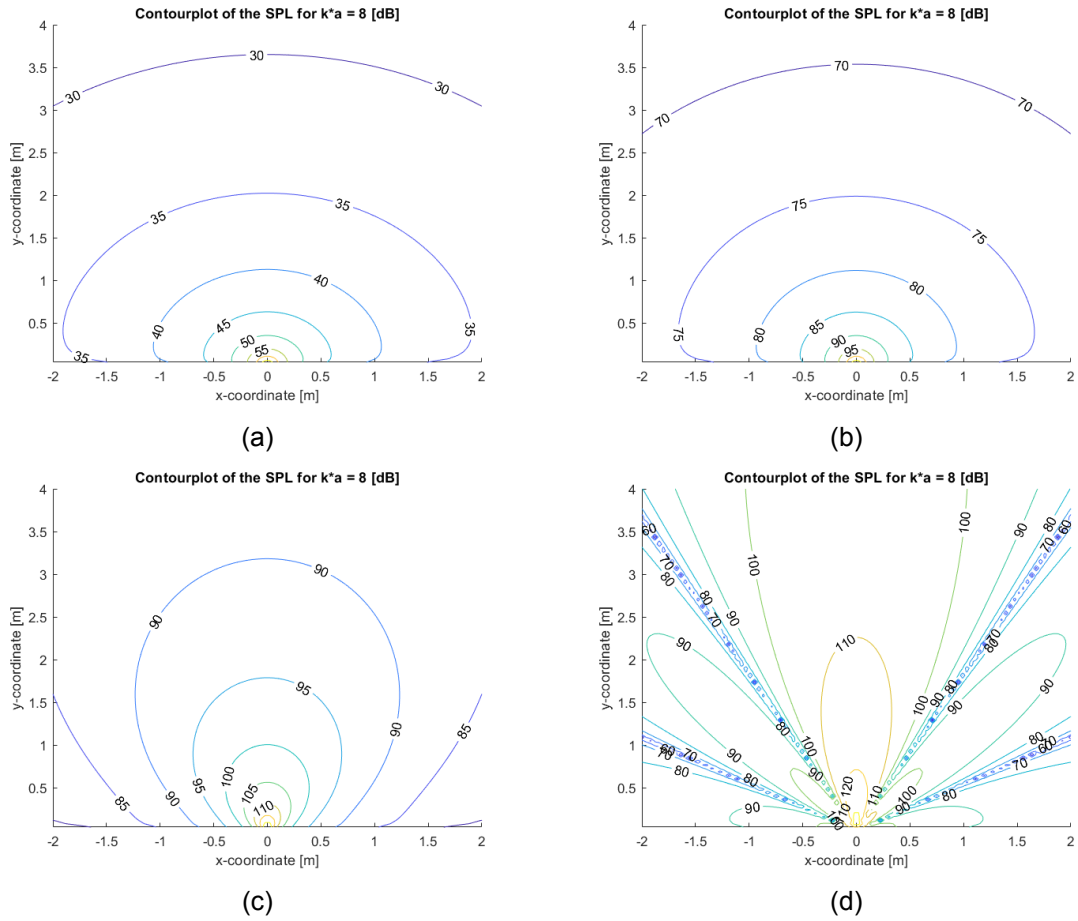

Figure 6.1: Contour plots of the SPL's for different values of ka: (a) 0.1 (b) 1 (c) 3 (d) 8 using equation 6.2.

$$p_\omega(r) = -ik\rho c\frac{e^{ikr}}{2r}u_\omega a^2 \tag{6.4}$$

This approximation is no longer valid at higher frequencies, as the movement of the plate is no longer pistonic above the first natural frequency.

The behaviour of equation 6.2 is very dependent on the value of ka. At low values the pressure distributes spherically around the source, whereas at higher values the pressure increases more in the direction normal to the piston. At even higher values the normal direction stays the highest, but "lobes" of higher SPL's start forming, as can be seen in figure 6.1

Given this behaviour, as long as the value of ka does not exceed 1 by far the result of equation 6.2 does not change strongly depending on the exact position of the observer, whereas at higher values it does change strongly. Also slight deviations in parameters have less influence on the SPL's at specific positions for lower values of ka. From this it can be concluded that equation 6.2 is best used to approximate the SPL's generated with the sound source at lower values of ka. As the first problematic natural frequency of the system occurs around 500Hz, corresponding to a value of $ka = 1.16$, this approximation is accurate for the used frequency range.

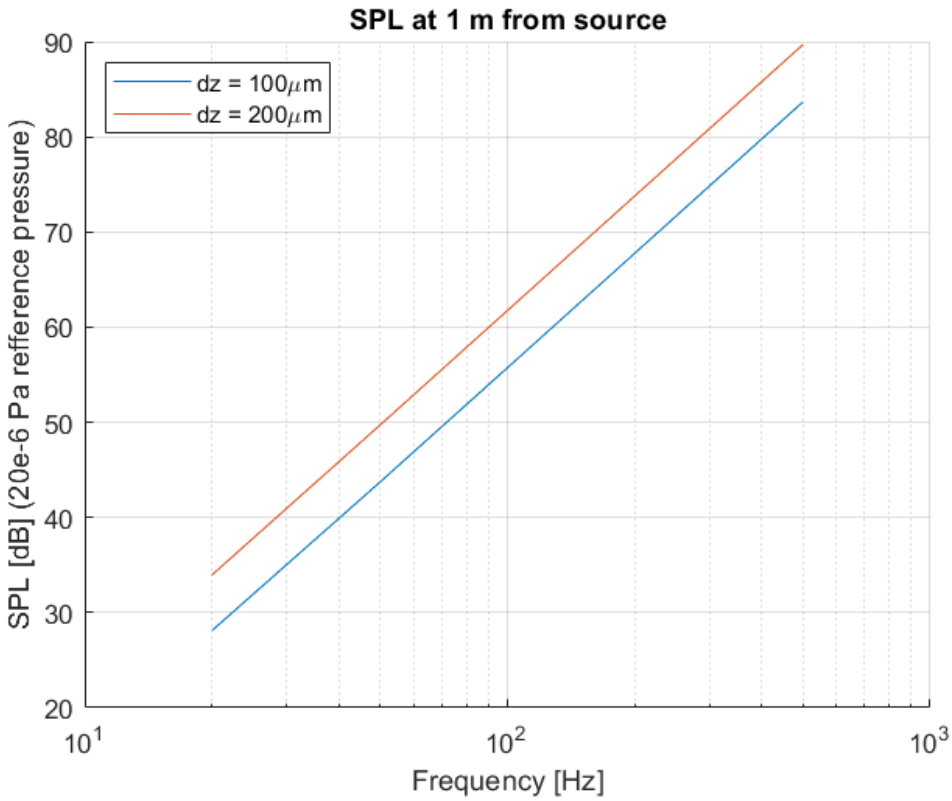

Figure 6.2: Sound pressure levels at 1 meter from the source for a displacement of 100μm and 200μm for frequencies between 20-500Hz and a piston surface area of $0.06237m^2$.

6.2 Acoustic validation

This model can be used to predict SPL's at various ranges and angles from the source for any displacement of the piston. Using this, the effect of the requirement of 100μm displacement can be predicted, which is shown in figure 6.2. It can clearly be seen that the SPL increases with increasing frequency. For a higher displacement, the the SPL's are higher. Doubling the displacement increases the SPL by 6dB.

Simulations show that a piezo displacement of 60μm corresponds to 200μm displacement of the plate. During this movement the stresses do not exceed 0.5GPa, which is below the fatigue limit. The actual displacement of the piezo depends on the exact type, shape and blocking force, though a displacement of roughly 0.1% is feasible [5]. This means that in the design there is enough space for a piezoelectric actuator that can produce the 200μm displacement of the plate.

7 MANUFACTURING

In the previous chapters the theoretical side of the design are extensively discussed and many parts are optimised. In this chapter the process of realising the mechanism is discussed. From this it will become clear that there is a big gap between what is optimal and what is available in time.

7.1 Piezo

In the design phase, a piezoelectric actuator was designed to have desirable dimensions and properties. In order to find realistic properties, multiple available piezos were looked up online. After the design was done, a piezo had to be purchased to realise the mechanism. In this process, it turned out that the availability of piezos was more limited than initially thought. Finding a piezo of similar dimensions, stroke and of sufficient blocking force, which was available within a reasonable time and within available budget turned out not to be a trivial task.

Through an extensive search of available piezos of different suppliers a shortlist was made, visible in figure 7.1. For missing information, specifically quotes and delivery times contact was sought with the suppliers. Based on the reactions and non-reactions, a choice was made to order 2 PK4GYP2 actuators from Thorlabs [36].

7.2 Sandwich plate

For the sandwich plate, the face plates had to be manufactured and the core material had to be ordered. As the most lightweight core materials were deemed best for the task, these were selected to be used. As the suppliers did not have a webshop, a quote was requested through

1	Type name	Supplier	Stroke	Blocking force	Dimensions	Amount required	Price	Delivery time	Other remarks
2	PSt150/10 × 10/20	AliExpress	28µm	7000N	10x10x18mm	3	€2171,73 (3x723,91)	~4 weeks	
3	PSt150/7*7/20H	AliExpress	20µm		7,1x7,1x18mm	4	€1348,44 (4x337,11)	~3 weeks	
4	AHB151C362WD1-A0LF	KEMET (YAGEO)	140µm	3600N	20x142mm (round)	1	?	?	
5	AHB101C801WD1-A0LF	KEMET (YAGEO)	103µm	800N	13x142mm (round)	1	?	?	
6	AE0505D44H40DF	KEMET (YAGEO)	42µm	850N	5x5x40mm	2	$521,14 (2x260,57)	37 weeks	
7	NAC2021-70-A01	Noliac (Cts)	112,2µm	2060N	7x7x70mm	1	€1199,-	8 weeks	
8	P-885.95	PI	30µm	900N	11,2x40,5mm (round)	3	?	?	Connections topside
9	P-840.6	PI	90µm	1000N	12x122mm (round	1	?	?	Lompe connectors
10	P-887.91	PI	32µm	1850N	7x7x36mm	3	?	?	
11	P-885.91	PI	32µm	950N	5x5x36mm	3	?	?	
12	P-830.30	PI	45µm	1000N	?x58mm	2	?	?	
13	P-088.781	PI	70µm	7500N	16x77mm (round)	1	?	?	
14	P-080.391	PI	25µm	850N	8x36mm (round)	3	?	?	
15	PA 90/14 SG	piezosystemjena	80µm	850N	14x109mm (round)	1	?	?	
16	PK2FVP2	Thorlabs	44,8µm	1000N	5x5x39,8mm	2	€423,44 (2x211,72)	4 days	Connections topside
17	PK4GA7P2	Thorlabs	100µm	1960N	7x7x90mm	1	€ 568,50	4 days	Connections topside
18	PK4GYP2	Thorlabs	38µm	1960N	7x7x36mm	2	€343,- (2x171,50)	4 days	Connections topside

Figure 7.1: A shortlist of available piezos with properties similar to the required properties. In red the reasons for dismissing, in yellow factors contributing negatively to the rating of the piezo. Based on this, the piezo in the last line was chosen. Properties found at the websites of suppliers and/or through communication with the suppliers.

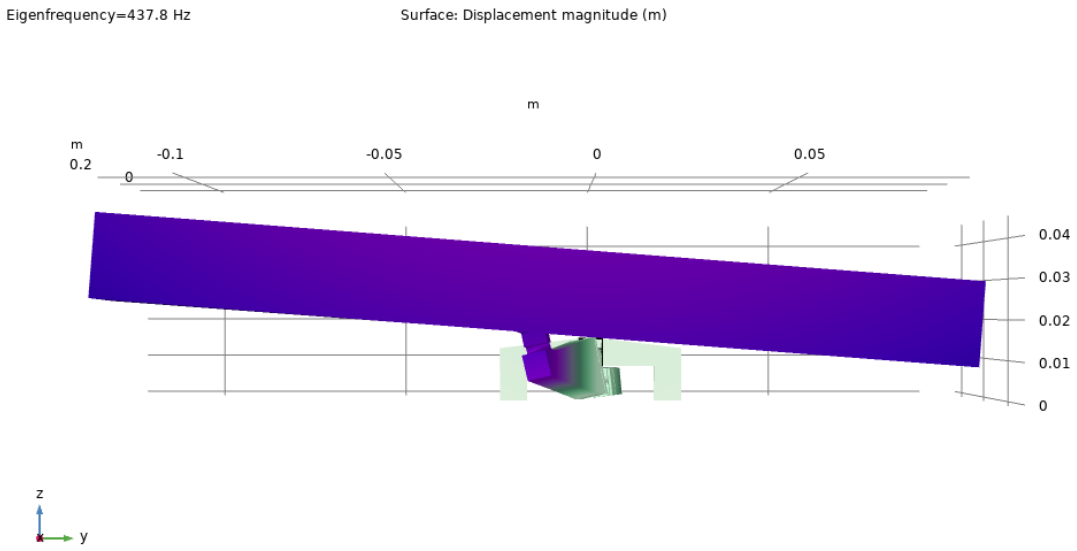

Figure 7.2: By reducing the thickness of the conversion mechanism from 10mm to the available 6mm, an extra mode is introduced. This mode corresponds to a natural frequency below the original first natural frequency, thereby lowering the effective frequency range of the source.

the applicable channels on their websites. Unfortunately no response was received. This lead to settling for a slightly heavier, but available core material. Due to time constraints, the sandwich plate of [33] is reused.

7.3 EDM parts

For the machining of the conversion mechanism and the pretension mechanism, a supplier was sought. Multiple machine shops were contacted for a quote. Unfortunately only one potential supplier responded, mentioning that production would take at least 8 weeks, giving no upper limit. This was deemed to be too long.

At the university, the department TCO does have EDM capacity. This department has manufactured parts for master theses before, so they were contacted. Though they would not be able to reach the same tolerances that were advertised by commercial suppliers, this was deemed good enough. After machining, the parts would have to be measured to model the performance more accurately.

The chosen material, Stavax®, was not available in the required dimensions for the conversion mechanism. Simulations were conducted on slight adaptations to fit the available dimensions, but these severely affected the performance. The most suitable option would be to reduce the thickness of the conversion mechanism from 10 to 6mm. Simulations showed that this would introduce and extra natural mode within the use range, thereby reducing the frequency range for which the source can be used. This mode is visible in figure 7.2.

From this it was concluded that the 6mm thick piece of Stavax® was not suitable. Some other materials were available at TCO in the right dimensions, but the exact properties of these materials was unknown. The available materials were DIN 1.2510, DIN 1.2842 and DIN 1.2767. Properties of these materials depend on hardness grade and other treatments, and information on these varies wildly depending on which source is used.

The most important factor for choosing the right material in this case is the fatigue strength, as this is the limiting factor in the design. This strength is between 35% and 50% of the yield strength [31]. Therefore the highest yield strength material is chosen, which is DIN 1.2510, at 1350 MPa. This material has a Young's modulus of 193GPa, and thus the system behaves slightly different. By reducing the maximum allowable stroke of the piezo, simulations show that the fatigue limit will not be exceeded during use. This does slightly reduce the acoustic performance, decreasing the achievable SPL's.

For the pretension mechanism the available dimensions of Stavax® were sufficient. Therefore no adjustments were made to this.

7.4 Supports

The supports for the frame were milled from a solid piece of aluminium. The in the converter two slots were milled for the supports to fit in.

7.5 Box

In the design phase, a box made of MDF was chosen because of its mechanical and acoustic properties. For demonstration purposes however, is not desirable, as it would provide no way to view what is going on inside the box. Therefore a choice was made for perspex as box material. This does affect the damping properties of the box. Due to time constraints, the box of [33] is reused. Holes and other remains from previous use have been covered up to negate their potential effects.

7.6 Amplifier

To power the system an amplifier is used in combination with a transformer. Transformer transforms 230V to 115V and the amplifier is powered by 115V. The amplifier is able to supply AC and a DC offset.

7.7 Assembly

The piezos were glued in the pretension mechanism using Araldite® two component glue. In order to do this the pretension mechanism was strained using custom milled aluminium clamp which was fixed in the head of a drill press. After 24 hours of drying, the actuation assembly was glued in the converter, again using Araldite®. Again after 24 hours of drying, the supports were attached to the converter. Next a hole was drilled in the box through which a pin was placed that connected to a hole drilled in the converter. These were again glued together. Then the sandwich plate was glued to the converter and after drying the rubber suspension was added using double sided tape. After this, the wires of the piezos were connected to the amplifier.

The connection between the rubber and the plate failed before testing. This was due to the fact that the height of the reused perspex box was less than expected. Because of this, the edge of the plate was higher than the edge of the box, causing the rubber suspension to be curved instead of flat. Combining this with the fact that the reused rubber had dried out a little bit, made that the double sided tape was not strong enough. While attempting to solve this, the connection between the plate and the converter also failed. Because of this both connections

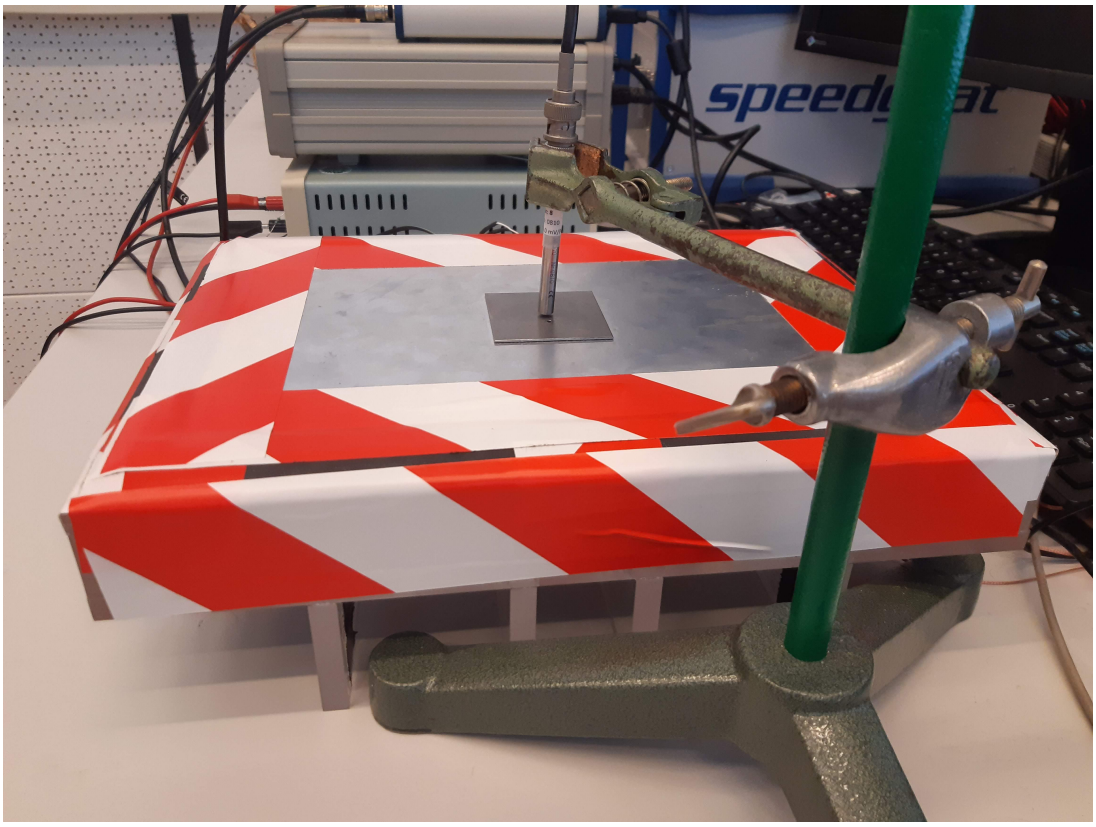

Figure 7.3: The final prototype with microphone. The red-white tape was improvised to fix failed connections.

needed renewal.

Because of severe time constraints, the chosen solution was neither very good, nor glamorous. The chosen solution consisted of removing the old glue and tape, renewing the glue and using strong air tight tape on both sides of the rubber strips to attach them to the plate and box. Because of this, the stiffness of the suspension became much higher than designed. Also some pretension was most likely added because the tape was pulled while attaching in order to make the connection air tight. As an unfortunate side-effect of using the tape, most of the perspex box was covered, although the downside of the box was still transparent. The manufactured prototype can be seen in figure 7.3.

8 VALIDATION

In order to test if the mechanism has been modelled correctly and behaves as expected, multiple validation tests have been conducted for both the mechanical behaviour and the acoustic behaviour. The measurement setup can be seen in figure 8.1.

8.1 Displacement

The realisation of the mechanism differs from the simulation model. The exact material properties are not known for the conversion mechanism steel, the loaded properties of the piezo are not known exactly and slight miss-alignments might have been introduced during assembly. Because of this it is not possible to predict the exact displacement of the converter for a given voltage.

Simulations have been conducted for different displacements to find the maximum stresses in the mechanism. From this, maximum displacements have been determined for which fatigue is not a problem. The stroke of the actuators is $78\mu m$, which is amplified by the connector to around $200\mu m$ displacement of the sandwich plate. The maximum allowable stress in the manufactured model is through simulation in COMSOL found to be reached at a stroke of around $50\mu m$, which would translate to around $140\mu m$ displacement of the sandwich plate. A stroke of $50\mu m$, or $25\mu m$ for each piezo translates to around 100V of the maximum 150V. Therefore tests are not conducted for higher voltages.

8.2 Natural frequencies

To determine the natural frequencies of the mechanism a chirp is used. This is a signal of exponentially increasing frequency. Placing a microphone very close to the centre of the sound generator should reduce the influence of background noise. The microphone is placed at a distance of 5mm from the sandwich plate. By analysing the frequency response, the SPL's produced for each frequency, the natural frequencies can be found. As mode shapes corresponding to different natural frequencies have different stationary locations, the SPL is measured in multiple locations. These locations are the middle of the plate (mid-mid), the middle of the long edge (long-mid), the middle of the short edge (short-mid) and the corner of the plate (corner). Placing microphones at these locations should be sufficient to determine the first modes of the system.

In order to compare the results to the model, simulations were run on a model that was adapted to the changes in the manufactured prototype compared to the optimised model. The frequency response and natural frequencies and corresponding mode shapes are shown in figures 8.2 and 8.3a up to and including 8.3h.

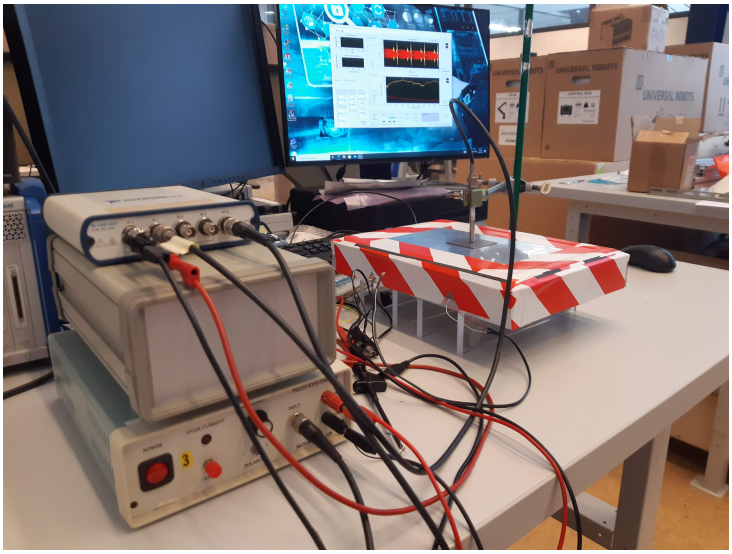

Figure 8.1: Overview of the final test setup with transformer, amplifier, measuring station, microphone, computer and acoustic source.

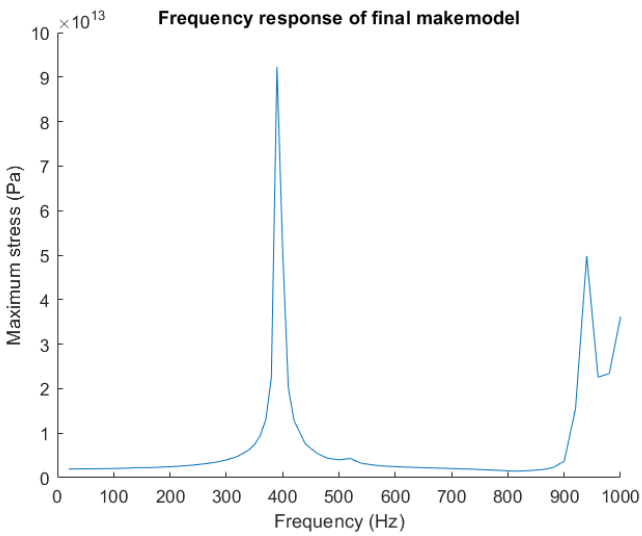

Figure 8.2: Simulated frequency response of the manufactured prototype. Note that the natural frequencies are significantly lower than in the optimised model of figure 5.26

.

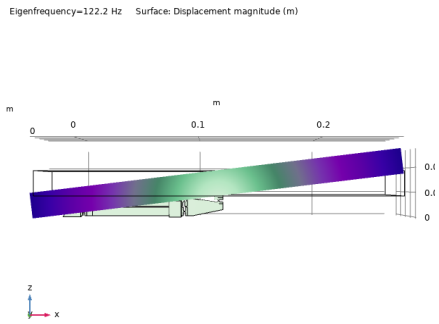

(a) 122Hz

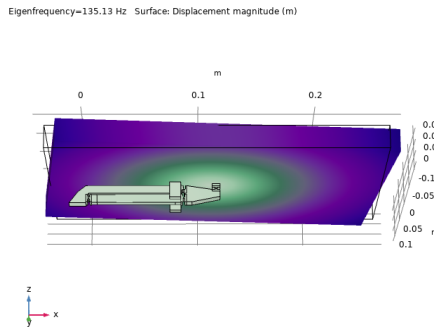

(b) 135Hz

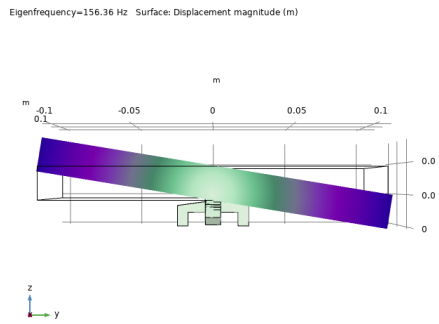

(c) 156Hz

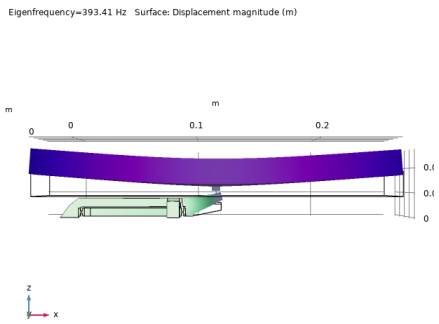

(d) 393Hz

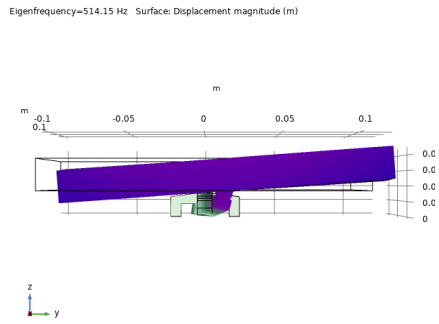

(e) 514Hz

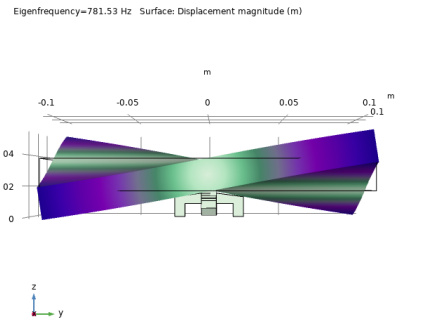

(f) 782Hz

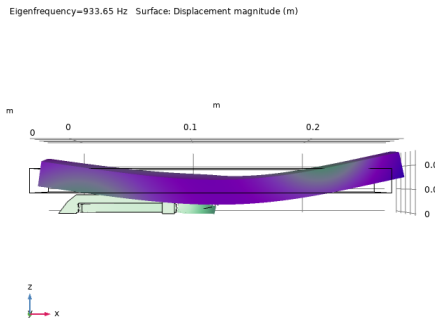

(g) 933Hz

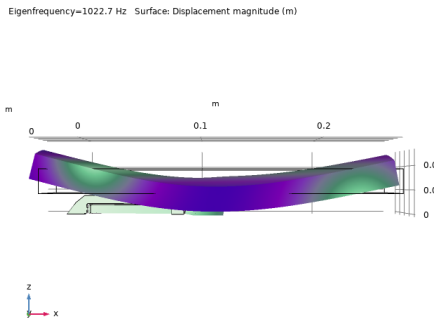

(h) 1023Hz

Figure 8.3: The first 8 simulated natural modes of the manufactured prototype with their respective natural frequencies.

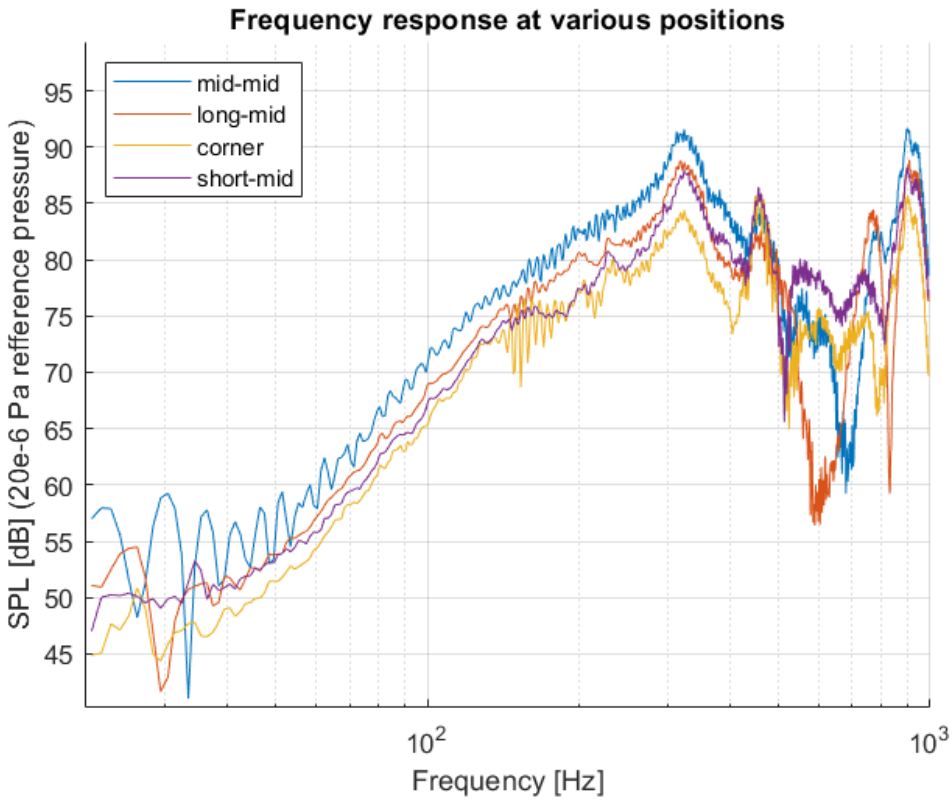

Figure 8.4: SPL measurements at multiple locations.

8.3 Acoustic behaviour

Having determined the natural frequencies of the system, a frequency range is determined for operation of the acoustic source. Using the model in Chapter 6, the expected SPL's can be determined for a given displacement of the sandwich plate. As the relation between voltage and displacement of the piezos is given by the manufacturer, a prediction can be made for the acoustic behaviour for given voltages.

8.4 Laser Vibrometer

A more accurate determination of the natural frequencies could be performed using a Scanning Laser Vibrometer. Due to time constraints this has not been performed.

8.5 Results

8.5.1 Determining natural modes and frequencies

First the mechanical behaviour was tested by placing the microphone in multiple locations, 5mm from the source. An exponential frequency sweep was conducted at 10V. The results are visible in figure 8.4.

From this figure the natural modes can be identified. All lines show a peak around 330Hz. This means that the plate excites as a whole, which corresponds to the mode shown in figure 8.3d, which is the large peak in figure 8.2. Because of the noisiness of the signal it is harder to determine the positions of the lower modes, but these lie somewhere between 120Hz and 180Hz.

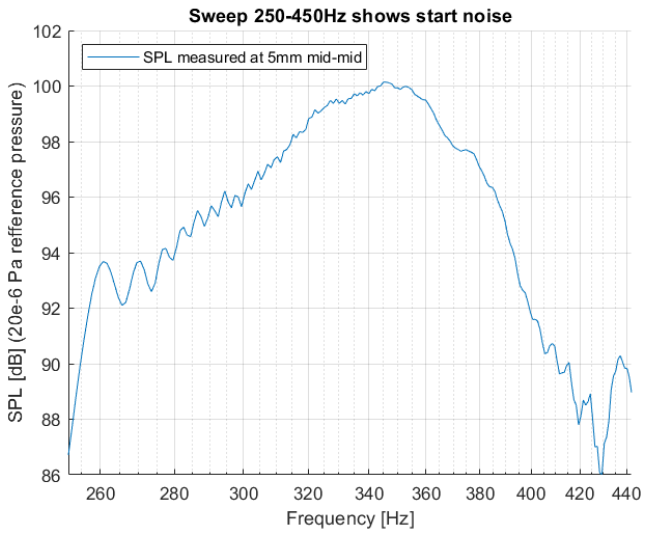

Figure 8.5: SPL measured in the middle of the plate, 5mm away, 10V, 250-450Hz. This test was performed to identify the first non-rigid-body mode more accurately. It was found around 340Hz.

These correspond to the rigid-body modes in figures 8.3a and 8.3c, where the middle of the plate is stationary and the sides are excited. These modes do not show up in figure 8.2. This is because in the simulation, the converter is placed exactly in the centre of the plate, which causes the sides to not be agitated and therefore to not have their movement amplified. In reality it was not possible to position the parts perfectly symmetrical which is why these modes are shown to be present in the response, though only a little. Above the first non-rigid-body mode, at 330Hz, the data becomes harder to read. A peak can be seen around 470Hz for all microphones, which corresponds to the mode in figure 8.3e. In this figure, the entire system ”wobbles”, causing all parts of the plate to excite. The higher frequency data is harder to read.

One thing that stands out is that the SPL in the middle of the plate is overall higher than those measured at the sides and corner. This is likely due to the fact that the source was not built in a wall but was standing alone. Therefore pressure could escape to the side and in the corner to both sides, which is why less pressure is measured at the microphone.

Based on these results, the sound source can be used up to around 300Hz without mechanical problems. Another test was performed to identify the first non-rigid-body mode more accurately by performing a chirp from 250Hz to 450Hz. This resulted in a natural frequency of around 340Hz, as visible in figure 8.5. This is lower than the predicted 390Hz from the COMSOL model. The exact cause of this was not found, but the manufactured prototype obviously differs quite a bit from the model. Also there are other factors with small influences that have not been taken into account in the model.

8.5.2 Noise

The data in both figures 8.4 and 8.5 is quite noisy. This has multiple causes. First there is the starting noise at the left of each graph. This is because the applied voltage is not changed to the desired voltage and frequency instantly, but is changed fast and with a small overshoot. This has been proven by performing an opposite chirp, which causes the extra noise to appear on the right side of the graph.

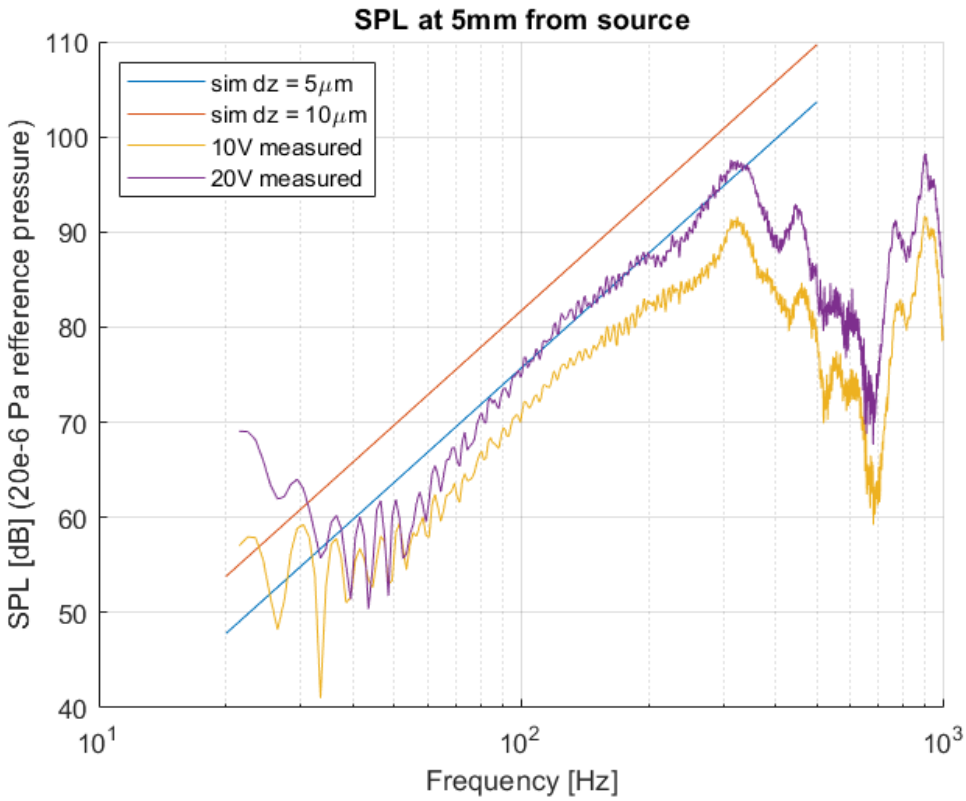

Figure 8.6: The measured SPLs for 10V and 20V plotted against the model results for $5\mu m$ and $10\mu m$ displacement. 10V should roughly translate to $5\mu m$ and 20V should translate to $10\mu m$ displacement of the plate.

The tests were not performed in an anechoic chamber due to time and availability constraints. Though the tests were performed while there was nobody else in the lab, background noise still affects the results.

8.5.3 Determining the acoustic behaviour

In order to determine the acoustic behaviour and compare it to the modelled result, the microphone was placed in the middle of the plate at 5mm distance. The intention was to perform multiple chirps at 10V, 20V, 30V, 40V, 50V, 60V, 70V, 80V, 90V and 100V. While performing the 30V chirp however, power was cut by the amplifier. The amplifier was supposed to be able to deliver up to 200V while the piezos were rated for a maximum of 150V. No solution to this cutting of power was found and multiple attempts were futile. Therefore unfortunately there is no data past 20V. The results of the 10V and 20V test compared to predicted results using the model in chapter 6 are shown in figure 8.6.

From this figure some things can be clearly seen. Firstly, the slope of the measured signals up to the first natural frequency corresponds to that of the model. Also the distance between both measured lines is for a large portion of the interval (80-400Hz) roughly equal to the distance between the two simulated lines. This means that the displacement is roughly doubled by doubling the voltage, which is to be expected.

The measured SPL's are lower than the expected SPL's by about 6dB. This means that the actual displacement is a factor 2 lower than the predicted displacement of the plate. This is partly

because the stroke of the piezo corresponding to a certain voltage is the unloaded stroke. As a pretension mechanism is applied, the stroke is not unloaded and therefore smaller than predicted. Also due to the improvised application of tape for air tightening the source, extra force is applied on the piezos, further reducing the stroke. The connection between the converter and the plate is very fragile and has failed already, so a rather thick layer of glue was applied, which dampens the excitation as well. If a measurement at 40V was performed, this would probably coincide roughly with the simulated line for $10\mu m$ displacement.

As the prediction from chapter 6 is only valid for pistonic motion, the prediction becomes worthless above the first natural frequency, which is why the measured curve deviates sharply from there on.

9 CONCLUSIONS AND RECOMMENDATIONS

9.1 Conclusions

Based on the results a number of conclusions can be drawn. First of all: thin sound source works as intended. The relevant natural modes and natural frequencies were predicted in the model, though they were predicted a little too high. The causes of this are manufacturing mistakes, changes in the design due to time and availability constraints and the fact that not all physical effects have been taken into account while modelling. The same goes for the roughly 6dB lower than expected SPL's.

The assignment was to improve upon the previous work. As the measured first natural frequency of the prototype was 340Hz and the first natural frequency of the previous work was 370Hz, this goal was not physically achieved. In simulation though, this was achieved, as 570Hz was predicted. Another goal was to make the converter less complex and better constrained. This was successfully achieved by reducing the number of bodies and hinges and by exactly constraining the converter.

Due to circumstances many concessions had to be made in manufacturing the prototype, which reduced the predicted natural frequency from 570Hz to 390Hz. If a small reduction in natural frequency from model to prototype (390Hz to 340Hz) can be extended to the optimised model, a first non-rigid-body mode natural frequency can be expected to be realisable around 500Hz, which is an improvement of over 35% from the previously realised 370Hz.

9.2 Recommendations

During this assignment some limitations were found and multiple ways were determined to improve upon the performed research. Some recommendations are:

- By utilising more computers, the design might be further optimised by trying more configurations. Optimisation algorithms might be applied to reduce the extra amount of computers needed.
- It is worth considering making a cutout in the bottom of the box around the mechanism. By doing this the thickness of the sound source might be reduced significantly.
- Somehow acquiring the materials and parts that were found in the optimisation of the design would significantly improve its performance.
- By enlisting the help of experienced personnel the manufacturing could be done faster and with less inaccuracies. Unexpected problems might be solved more elegantly as well.
- If the optimisation was cut-off earlier, there would have been more time for acquiring materials and manufacturing, perhaps resulting in a better performance.

- In similar designs the connection between the converter and the plate deserves more attention. Due to this oversight improvisation was required, possibly severely affecting performance.
- Performing the tests in an anechoic chamber reduces measurement noise resulting in clearer figures and more accurate conclusions.
- By performing more tests the noise can be filtered out and certainty about conclusions can be increased.
- Using a better amplifier can improve the results. This amplifier produced quite some noise and was not able to perform over 25V, while higher voltages are definitely interesting for determining how well a design performs.
- By using a Scanning Laser Vibrometer the natural frequencies and natural modes of a prototype can be determined more accurately than with microphones.

REFERENCES

[1] BERKHOFF, A. P. Sound generator, U.S. Patent US2010111351 (A1), 2010-05-06.

[2] Blackstock, D. *Fundamentals of physical acoustics*. Wiley, 2000. pages: 108-125.

[3] Budynas, W. C. Y. R. G. *Roark's formulas for stress and strain*. McGraw-Hill, 2002. pages: 765.

[4] Ceramics, P. Handling of piezo actuators, 4 2023. https://www.piceramic.com/fileadmin/user_upload/physik_instrumente/files/TEC/PI_Handling_Piezo_Actuators.pdf.

[5] Ceramics, P. Pi tds, 5 2023. https://www.physikinstrumente.com/fileadmin/user_upload/physik_instrumente/files/datasheets/P-216-Datasheet.pdf.

[6] Ceramics, P. Properties of piezoelectric actuators: Forces and stiffness, 4 2023. https://www.piceramic.com/en/expertise/piezo-technology/properties-piezo-actuators/forces-stiffnesses.

[7] CHUANHUI, H. W. D. W. S. Y. M. L. L. L. L. Sound barrier, CN206308633 (U) — 2017-07-07.

[8] Claeyssen, F. e. a. Amplified piezoelectric actuators: Static & dynamic applications. *Ferroelectrics 351(1)* (2007), 3–14.

[9] Composites, E. Core material aluminium honeycomb tds, 1 2023. https://media.easycomposites.co.uk/datasheets/EC-TDS-Aluminium-Honeycomb.pdf.

[10] DIETER, H. G. Flat panel loudspeaker, CN115699808 (A) — 2023-02-03.

[11] Eargle, J. *Loudspeaker Handbook*. Springer, 2011. pages: 132-140.

[12] Fan, M., and Fu, F. *Advanced high strength natural fibre composites in construction*. Woodhead Publishing, Ltd., 2017. pages: 333-373.

[13] Hansen, C. *Understanding Active Noise Control*. Spon, 2001. pages: 1-9.

[14] Heutschi, K. Acoustics i: sound field calculations, 5 2023. https://people.ee.ethz.ch/~isistaff/courses/ak1/acoustics-sound-field-calculations.pdf.

[15] Heywang, W., L. K., and Wersing, W. *Piezoelectricity: Evolution and future of a Technology*. Springer, 2008. pages: 157-180.

[16] Ho, J.-H., B. A. Flat acoustic sources with frequency response correction based on feedback and feed-forward distributed control. *The Journal of the Acoustical Society of America 137(4)* (2015), 2080–2088.

[17] Hobbie, R., and Roth, B. *Intermediate physics for medicine and biology*. Springer International Publishing, 2015. pages: 344.

[18] Kee Paik, J., T. A., and Sung Kim, G. The strength characteristics of aluminum honeycomb sandwich panels. *Thin-Walled Structures 35.3* (1999), 205–231.

[19] KOSAKU, T. S. M. Flat plate diaphragm, JPS61121700 (A) — 1986-06-09.

[20] Ltd., S. S. O. Acoustic foam technical specification, 5 2023. https://www.keepitquiet.co.uk/sound-absorbing-foam-technical-data/.

[21] MFG, N. M. I. Sound generators, NL6700473 (A) 1967-10-06.

[22] Noliac. Actuators for dynamic applications - tutorial, 5 2023. http://www.noliac.com/fileadmin/user_upload/documents/Tutorials/Tutorials_Actuator_2.pdf.

[23] Noliac. Tutorial piezo basics, 5 2023. http://www.noliac.com/fileadmin/user_upload/documents/Tutorials/Tutorials_Piezo_basics.pdf.

[24] Office, E. P. Epo faq procedure law, 5 2023. https://www.epo.org/service-support/faq/procedure-law.html.

[25] pakyangho. Flat type speaker having voice coil plate of three dimensional track type, KR101154253 (B1) — 2012-06-13.

[26] Philip M. Morse, K. U. I. *Theoretical Acoustics*. McGraw Hill Book Company, 1968. pages: 375-382.

[27] R. Lucinskis, C. M. Dynamic characterization of an amplified piezoelectric actuator. *Noliac A/S* (2016).

[28] Smith, S. *Flexures elements of Elastic Mechanism*. Gordon and Breach Science Publishers, 2000. pages: 32, 153-205.

[29] s.r.l., C. C. Nomex honeycomb - commercial, 1 2023. https://www.cel.eu/img_ins/files/nomex_com_Rev2_uk.pdf.

[30] SUKEHITO, S. Y. O. S. K. Honeycomb sandwich panel having soundproof characteristic, JP2007320289 (A) — 2007-12-13.

[31] Suresh, S. *Fatigue of materials*. Cambridge University Press, 1998. pages: 222.

[32] Swift, K. G., and Booker, J. D. *Manufacturing Process Selection Handbook*. Elsevier, 2013. pages: 205-207.

[33] Tajdari, F., Berkhoff, A., and de Boer, A. Numerical and experimental studies of a flat acoustic source that is actuated by an integrated flexure-based piezoelectric mechanism. *Journal of Sound and Vibration 482* (09 2020), 115435.

[34] Tajdari, F., Berkhoff, A., and de Boer, A. Numerical modeling of a flexural displacement-converter mechanism to excite a flat acoustic source driven by piezoelectric stack actuators. *Journal of Sound and Vibration 473* (02 2020), 115229.

[35] Tajdari, F., Berkhoff, A., Van der Zee, R., and de Boer, A. The influence of energy recovery on the overall efficiency of acoustic sources at low frequencies. *Journal of Sound and Vibration 485* (10 2020), 115548.

[36] Thorlabs. Pk4gyp2, 5 2023. https://www.thorlabs.com/thorproduct.cfm?partnumber=PK4GYP2.

[37] Uddeholm. Uddeholm stavax esr, 6 2023. https://www.uddeholm.com/app/uploads/sites/52/2019/11/Tech-Uddeholm-Stavax-ESR-EN.pdf.

[38] Xu, N., D. M., and Zhou, X. Analysis and design of symmetric notch flexure hinges. *Advances in Mechanical Engineering 9(11)* (2017).

[39] YIHANG, G. Novel color steel sandwich board, CN106760167 (A) — 2017-05-31.

[40] YUFENG, X. And sandwich board has good sound insulation effect, CN211973913 (U) — 2020-11-20.

[41] ZHUJIN, Z. Q. S. Moving coil flat composite coaxial loudspeaker, CN218336418 (U) — 2023-01-17.

[42] ZUKONG, H. Y. S. R. Z. Flattened loudspeaker and electronic equipment with same, CN217470276 (U) — 2022-09-20.

A APPENDICES

In this appendix the following things are included:

- A technical drawing of the converter
- A technical drawing of the prestress mechanism
- A literature study for types of acoustic sources

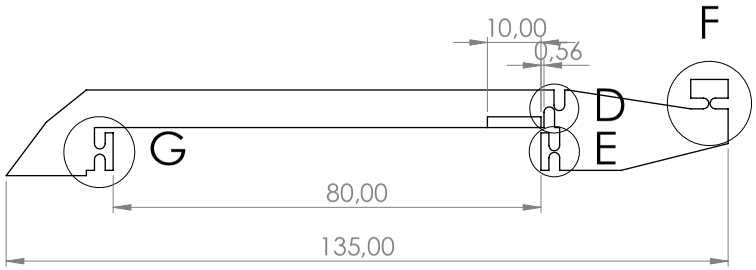

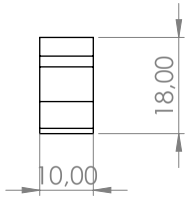

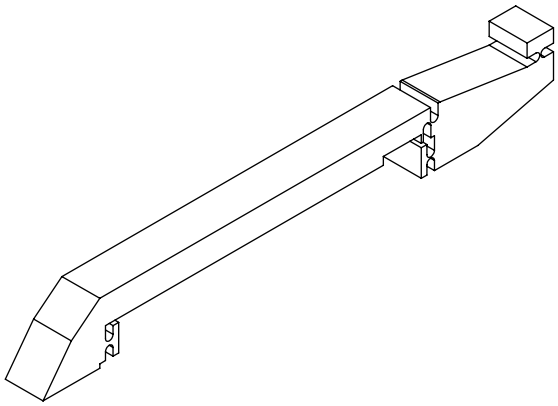

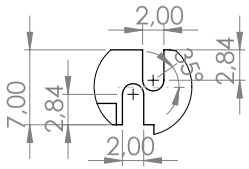

DETAIL D

SCALE 2 : 1

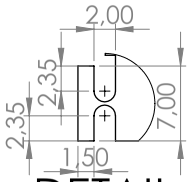

DETAIL E

SCALE 2 : 1

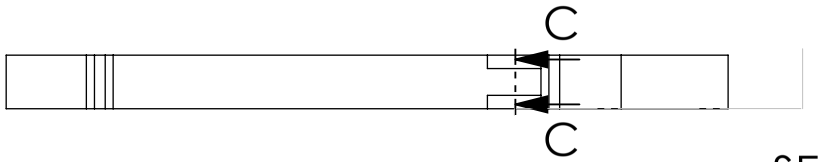

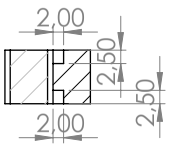

SECTION C-C

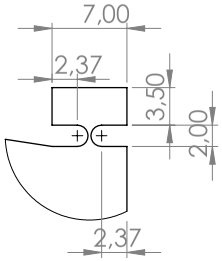

DETAIL F

SCALE 2 : 1

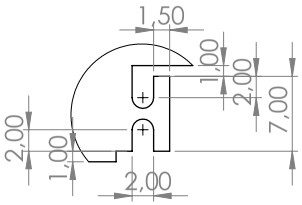

DETAIL G

SCALE 2 : 1

UNLESS OTHERWISE SPECIFIED: DIMENSIONS ARE IN MILLIMETERS SURFACE FINISH: TOLERANCES: LINEAR: ANGULAR:	FINISH:			DEBURR AND BREAK SHARP EDGES		DO NOT SCALE DRAWING	REVISION
	NAME	SIGNATURE	DATE			TITLE:	
DRAWN							
CHK'D							
APPV'D							
MFG							
Q.A				MATERIAL:		DWG NO.	A3
						Final_monolyth_with_support_c	
				WEIGHT:		SCALE:1:1	SHEET 1 OF 1

67

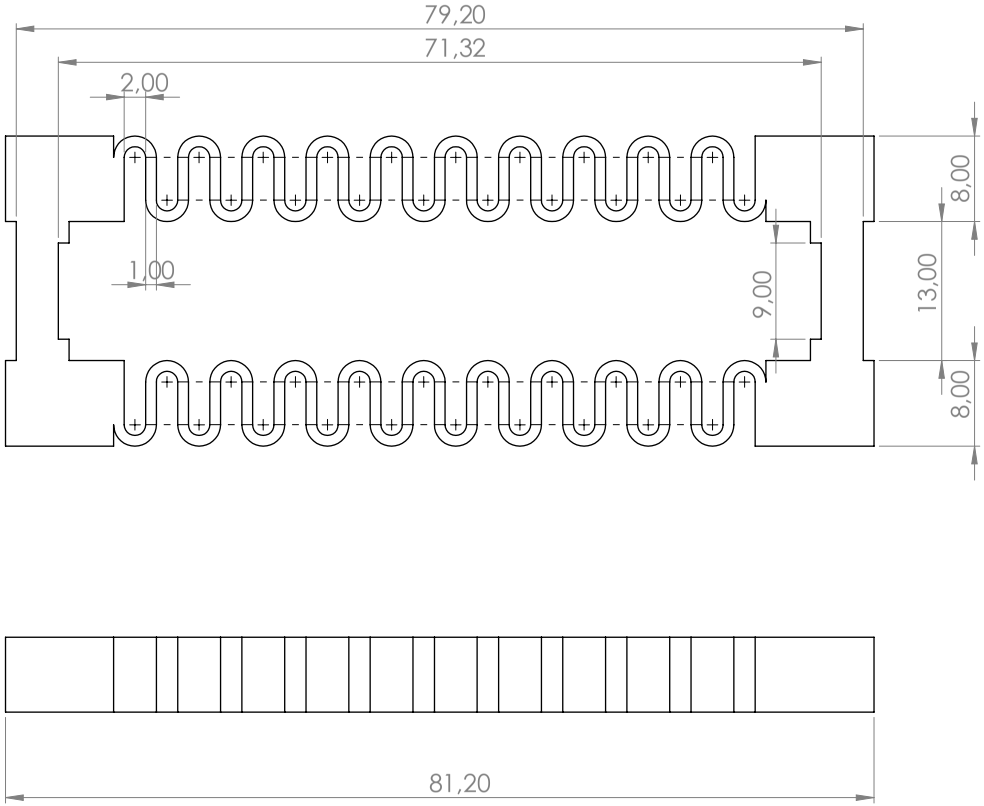

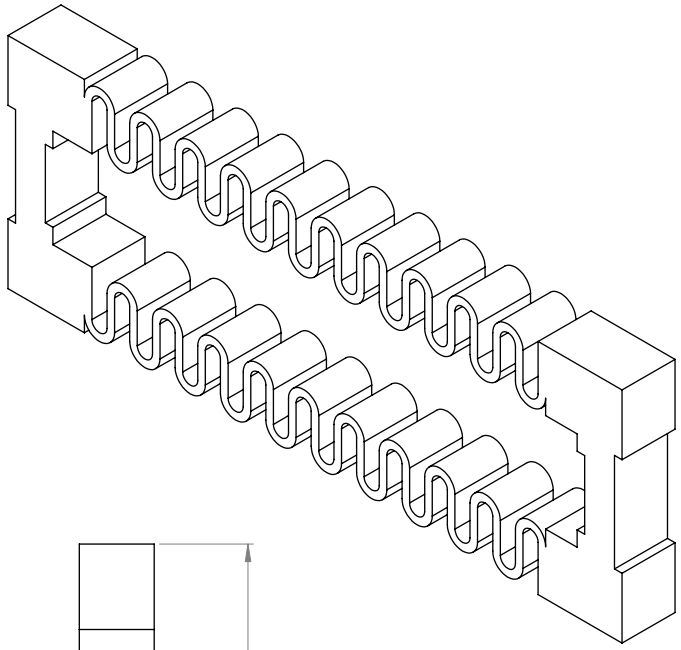

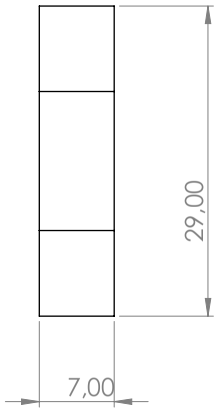

UNLESS OTHERWISE SPECIFIED: DIMENSIONS ARE IN MILLIMETERS SURFACE FINISH: TOLERANCES: LINEAR: ANGULAR:		FINISH:				DEBURR AND BREAK SHARP EDGES	DO NOT SCALE DRAWING	REVISION
	NAME	SIGNATURE	DATE				TITLE:	
DRAWN								
CHK'D								
APPV'D								
MFG								
Q.A				MATERIAL:			DWG NO.	A3
				WEIGHT:			SCALE:2:1	SHEET 1 OF 1

prestress_mechanism_0.8mm_finalised_addap

B TYPES OF ACOUSTIC SOURCES

There are many types of speakers, some well known, others less known. Each of these types has its pros and cons. Types differ in method of vibration generation and in how the vibration is converted to sound.

B.1 Dynamic loudspeaker

Probably the most well known and most used loudspeaker type is the dynamic loudspeaker. This type consists of a cone connected to a voice coil. The voice coil is constraint by a flexible suspension to only move in the axial direction. A permanent magnet surrounds the voice coil. By letting current flow through the voice coil, a magnetic field is generated which interacts with the field of the permanent magnet, generating a force on the voice coil, the direction depending on the direction of the current. By applying an active current of the desired frequency, the voice coil moves the cone at that frequency, which in turn pushes the air to create sound [11]. A schematic of a simple version of this loudspeaker is visible in figure B.1. These types of speakers are relatively cheap and easy to manufacture.

B.2 Piezo speaker

Another type of loudspeaker is the piezo speaker. This type consists of a stiff conical diaphragm to which a piezo element is attached. This element can bend, twist or warp if an electrical signal is applied to it. This slight movement drives the diaphragm, which forces the air next to it to move at the applied frequency. This speaker type has been used for a long time in cheap microphones and high frequency loudspeakers. On-axis output can be extended to higher frequencies than

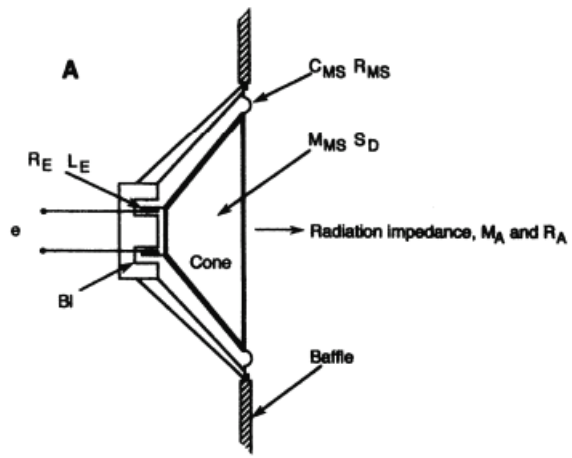

Figure B.1: Schematic of a simple dynamic loudspeaker [11].

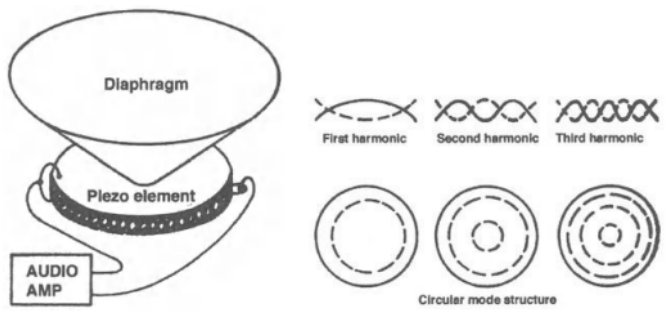

Figure B.2: Schematic of a piezo speaker with next to it the natural modes. [11].

the resonance frequency of the diaphragm, but off-axis this does not work [11]. A schematic of this type of speaker is visible in figure B.2.

B.3 Electrostatic

Another well known type of loudspeaker is the electrostatic loudspeaker (ESL). In this type, a conductive diaphragm is suspended between two electrodes. By applying a positive charge to one electrode and a negative charge to the other, the diaphragm can be moved by applying either a positive or a negative charge to it. By alternating the charge on the diaphragm at a given frequency, the air next to it is moved at that frequency and sound is generated [11].

As the diaphragm in this type is very lightweight and flexible, very little energy is required to drive it and resonance frequencies are not as relevant as in other types. On the other hand, as the displacement is very small, it has trouble producing bass frequencies, which can only be compensated by having a large surface area. These speakers are therefore often quite large. This type of loudspeaker is also very susceptible to distortion because of changes in humidity. [11]. A schematic is visible in figure B.3.

B.4 Distributed mode loudspeaker (DML)

A potentially much thinner type of loudspeaker is the distributed mode loudspeaker. This is a flat panel loudspeaker. A large flat panel speaker driven in the centre would either require a very stiff panel or it would have problems with resonance frequencies in the panel. In DML's this is solved by driving the panel off-centre. By carefully choosing the position of the driver and picking the right panel mass and driver mass, the operating bandwidth can be determined. This panel will have low frequent modes that limit its operating bandwidth, but above that it should have a fairly broad bandwidth, limited by the following equations [11]:

$$f_{max} = \frac{R_p}{2\pi M_c} \tag{B.1}$$

$$f_{min} = \frac{R_p}{2\pi M_m} \tag{B.2}$$

in which f_{min} and f_{max} are the minimum and maximum operating frequencies, respectively, R_p is the radiation resistance of the panel, M_c is the driven mass and M_m is the mass of the driver [11]. This system can be viewed in figure B.4.

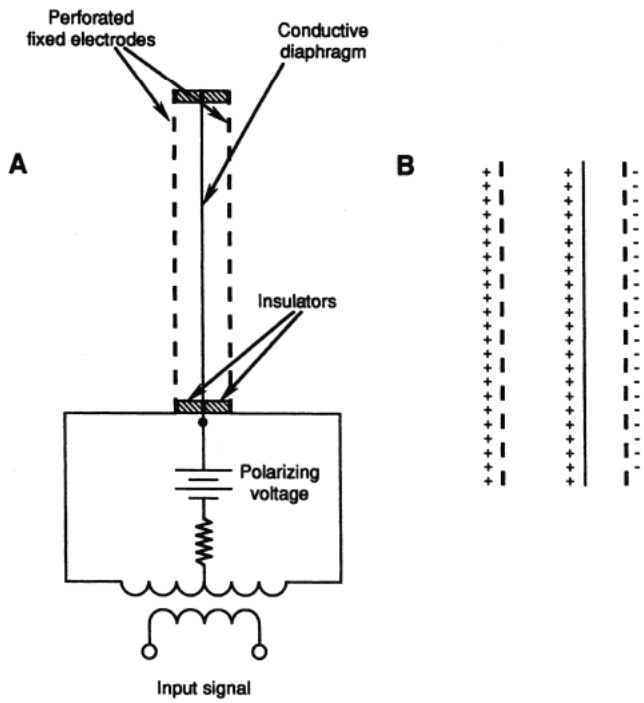

Figure B.3: Schematic of an electrostatic array speaker. On the right the charge to the electrodes and diaphragm is shown with the resulting movement of the diaphragm to the right. [11].

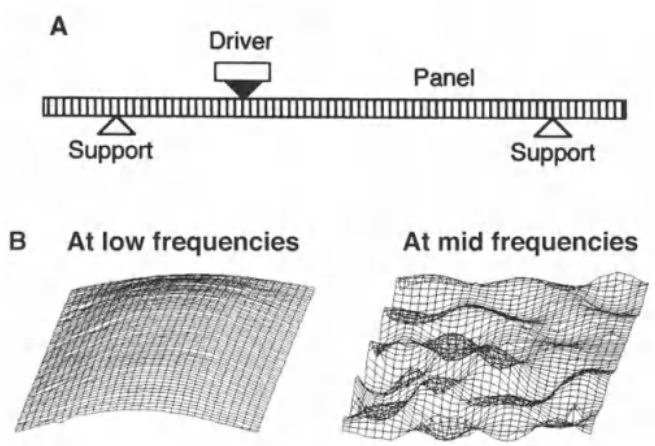

Figure B.4: Schematic of a distributed mode loudspeaker (DML). (A) shows the working principle, (B) shows the behaviour at low- and mid-frequencies [11].

B.5 Alternatives

These were some of the most common types of loudspeakers. Many other types have been theorised and tried. In specific applications others are being used. Some other types include: horn loudspeakers, in which a horn shape amplifies the sound; ionised air devices, in which the air itself is vibrated through electrical charge; air motion transformers, in which a folded membrane pushes out air when charged.